

ผลของภาวะการขึ้นรูปต่อการแยกตัวที่ผิวหน้าของพอลิเมอร์ผสมระหว่าง s-BPDA/ODA พอลิอิมมิดกับบล็อกโค
พอลิอิมมิดที่มีซิลิโคนเป็นองค์ประกอบ



นางสาว วันเพ็ญ เบญจพันธ์

สถาบันวิทยบริการ

จุฬาลงกรณ์มหาวิทยาลัย

วิทยานิพนธ์นี้เป็นส่วนหนึ่งของการศึกษาตามหลักสูตรปริญญาวิศวกรรมศาสตรมหาบัณฑิต

สาขาวิชาวิศวกรรมเคมี ภาควิชาวิศวกรรมเคมี

คณะวิศวกรรมศาสตร์ จุฬาลงกรณ์มหาวิทยาลัย

ปีการศึกษา 2548

ISBN 974-53-2570-8

ลิขสิทธิ์ของจุฬาลงกรณ์มหาวิทยาลัย

EFFECTS OF PROCESSING CONDITION ON THE SURFACE SEGREGATION OF *s*-BPDA/ODA
POLYIMIDE AND SILICONE-CONTAINING BLOCK COPOLYIMIDE BLENDS



Miss Wanpen Benjapan

สถาบันวิทยบริการ
จุฬาลงกรณ์มหาวิทยาลัย

A Thesis Submitted in Partial Fulfillment of the Requirements
for the Degree of Master of Engineering Program in Chemical Engineering

Department of Chemical Engineering

Faculty of Engineering

Chulalongkorn University

Academic Year 2005

ISBN 974-53-2570-8

Thesis Title EFFECTS OF PROCESSING CONDITION ON THE SURFACE SEGREGATION
OF s-BPDA/ODA POLYIMIDE AND SILICONE-CONTAINING BLOCK
COPOLYIMIDE BLENDS

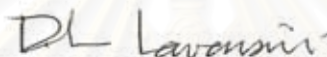
By Miss Wanpen Benjapan

Field of Study Chemical Engineering

Thesis Advisor Assistant Professor Sarawut Rimdusit, Ph.D.

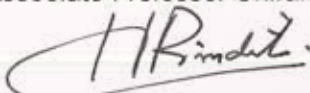
Thesis Co-advisor Associate Professor Suttichai Assabumrungrat, Ph.D.

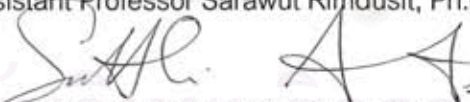
Accepted by the Faculty of Engineering, Chulalongkorn University in Partial
Fulfillment of the Requirements for the Master's Degree



..... Dean of the Faculty of Engineering
(Professor Direk Lavansiri, Ph.D.)

THESIS COMMITTEE


..... Chairman
(Associate Professor Chirakarn Muangnapoh, Dr. Ing.)


..... Thesis Advisor
(Assistant Professor Sarawut Rimdusit, Ph.D.)


..... Thesis Co-advisor
(Associate Professor Suttichai Assabumrungrat, Ph.D.)


..... Member
(Associate Professor Siriporn Damrongsakkul, Ph.D.)


..... Member
(Assistant Professor Varong Pavarajarn, Ph.D.)

นางสาววันเพ็ญ เบญจพันธ์ : ผลของภาวะการขึ้นรูปต่อการแยกตัวที่ผิวหน้าของพอลิเมอร์ผสมระหว่าง s-BPDA/ODA พอลิอิมิดกับบล็อกโคพอลิอิมิดที่มีซิลิโคนเป็นองค์ประกอบ. (EFFECTS OF PROCESSING CONDITION ON THE SURFACE SEGREGATION OF s-BPDA/ODA POLYIMIDE AND SILICONE-CONTAINING BLOCK COPOLYIMIDE BLENDS) อ. ที่ปรึกษา : ผศ.ดร. ศราวุธ ริมดุสิต, อ. ที่ปรึกษาร่วม : รศ.ดร. สุทธิชัย อัสสะบำรุงรัตน์, 86 หน้า. ISBN 974-53-2570-8

งานวิจัยนี้มีจุดมุ่งหมายเพื่อศึกษาผลของภาวะการขึ้นรูปต่อการแยกเฟสของ 3,3',4,4'-ไบฟีนิลเตตระคาร์บอไนล์ไดอะไมด์ (s-BPDA)/4,4'-ไดอะมิโนไดฟีนิลอีเทอร์ (ODA) พอลิอิมิดกับบล็อกโคพอลิอิมิดที่มีซิลิโคนเป็นองค์ประกอบ (BSF30) พอลิอิมิดสังเคราะห์ได้จากกระบวนการสองขั้นตอนซึ่งในขั้นตอนแรกจะได้พอลิเอมิกแอซิด (PAA) ซึ่งเป็นพอลิเมอร์ที่อยู่ในตัวทำละลาย N-methyl-2-pyrrolidinone (NMP) ในการผสมพอลิเอมิกแอซิดกับบล็อกโคพอลิอิมิดที่มีซิลิโคนเป็นองค์ประกอบจะทำการเปลี่ยนแปลงปริมาณของบล็อกโคพอลิอิมิดที่มีซิลิโคนเป็นองค์ประกอบ และทำการขึ้นรูปเป็นฟิล์มโดยใช้กระบวนการสร้างหมึกโม่ด้วยความร้อน จากผลการทดลองด้วยเครื่อง DSC ฟิล์มผสมพอลิอิมิดจะแสดงอุณหภูมิเปลี่ยนสถานะคล้ายแก้วสองตำแหน่งด้วยกัน ตำแหน่งแรกที่อุณหภูมิ 165 องศาเซลเซียส แสดงถึงส่วนของบล็อกโคพอลิอิมิดที่มีซิลิโคนเป็นองค์ประกอบ และที่อุณหภูมิ 272 องศาเซลเซียส แสดงถึงส่วนของ s-BPDA/ODA พอลิอิมิด และจากผลการทดลองจากเครื่อง DSC, TGA และ DMA พบว่าที่อัตราส่วนของบล็อกโคพอลิอิมิดที่มีซิลิโคนเป็นองค์ประกอบในปริมาณน้อยๆ เช่นที่ 0.5-5 phr ฟิล์มผสมจะไม่แสดงถึงผลจากการเติมบล็อกโคพอลิอิมิดที่มีซิลิโคนเป็นองค์ประกอบ เนื่องจากมีปริมาณของบล็อกโคพอลิอิมิดที่มีซิลิโคนเป็นองค์ประกอบน้อยมาก การทดสอบลักษณะที่ผิวของฟิล์มผสมโดยใช้เทคนิคการวัดมุมสัมผัส, เครื่อง Atomic force microscope (AFM), X-ray photoelectron spectroscopy (XPS) และ Attenuated total reflection Fourier transform infrared (ATR-FTIR) จากผลการทดลองพบว่าพอลิเมอร์ผสมระหว่าง s-BPDA/ODA พอลิอิมิดกับบล็อกโคพอลิอิมิดที่มีซิลิโคนเป็นองค์ประกอบเกิดการแยกตัวที่ผิวหน้าขึ้น และลักษณะของฐานรองรับที่ใช้ในการขึ้นรูปฟิล์มผสมจะมีผลต่อการแยกตัวที่ผิวหน้าของฟิล์มผสม โดยซิลิโคนในส่วนของบล็อกโคพอลิอิมิดที่มีซิลิโคนเป็นองค์ประกอบซึ่งมีความเป็นขั้วต่ำ จะเคลื่อนตัวขึ้นไปอยู่ที่ผิวหน้าด้านที่สัมผัสกับอากาศ และ s-BPDA/ODA พอลิอิมิดจะอยู่ด้านที่ติดกับกระจกเนื่องจากมีความเป็นขั้วสูงกว่าบล็อกโคพอลิอิมิดที่มีซิลิโคนเป็นองค์ประกอบ พฤติกรรมการแยกตัวที่ผิวหน้าสามารถเห็นได้ชัดเจนด้วยเทคนิค ATR-FTIR เมื่ออัตราส่วนของบล็อกโคพอลิอิมิดที่มีซิลิโคนเป็นองค์ประกอบมากพอ สำหรับที่สัดส่วนของบล็อกโคพอลิอิมิดที่มีซิลิโคนเป็นองค์ประกอบในปริมาณน้อยๆ เช่นที่ 0.5-5 phr จะได้ชัดเมื่อใช้เครื่อง XPS เมื่อวัดมุมสัมผัสของผิวฟิล์มผสมด้วยน้ำโดยใช้เครื่อง contact angle พบว่าที่ผิวฟิล์มผสมด้านที่สัมผัสกับอากาศมีมุมสัมผัสของน้ำสูงกว่าคือประมาณ 102° เนื่องจากส่วนที่มีความเป็นขั้วต่ำได้เคลื่อนตัวขึ้นไป สำหรับด้านที่สัมผัสกับกระจกค่ามุมสัมผัสของน้ำจะมีค่าประมาณ 77° พฤติกรรมนี้เป็นการยืนยันว่าเกิดการแยกตัวที่ผิวหน้าของฟิล์มผสมระหว่าง s-BPDA/ODA พอลิอิมิดกับบล็อกโคพอลิอิมิดที่มีซิลิโคนเป็นองค์ประกอบ

ภาควิชา.....วิศวกรรมเคมี.....

สาขาวิชา.....วิศวกรรมเคมี.....

ปีการศึกษา.....2548.....

ลายมือชื่อนิสิต..... กัญเพ็ญ เบญจพันธ์

ลายมือชื่ออาจารย์ที่ปรึกษา.....

ลายมือชื่ออาจารย์ที่ปรึกษาร่วม.....

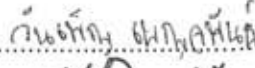
#4670488821: MAJOR CHEMICAL ENGINEERING


KEY WORD: POLYIMIDE/ IMMISCIBLE BLENDS/ SURFACE SEGREGATION/


PHASE SEPARATION

WANPEN BENJAPAN: EFFECTS OF PROCESSING CONDITION ON THE SURFACE SEGREGATION OF s-BPDA/ODA POLYIMIDE AND SILICONE-CONTAINING BLOCK COPOLYIMIDE BLENDS. THESIS ADVISOR: ASST. PROF. SARAWUT RIMDUSIT, Ph.D., THESIS CO-ADVISOR: ASSOC. PROF. SUTTICHAJ ASSABUMRUNGRAT, Ph.D., 86 pp. ISBN 974-53-2570-8.

This research aims to investigate the effect of processing condition on surface segregation of polyimide blends based on 3,3',4,4'-biphenyltetracarboxylic dianhydride (s-BPDA)/4,4'-diaminodiphenylether (ODA) polyimide and silicone-containing block copolyimide (BSF30). The polyimide was synthesized by a conventional two-step method via poly(amic acid) (PAA) precursor in N-methyl-2-pyrrolidinone (NMP) solvent. These polyimide blends, having various compositions of the silicone-containing block copolyimide, were processed by the solution casting method then undergone thermal imidization to yield the solid films. The DSC thermograms of the polyimide blends disclose the glass transition temperatures of BSF30 to be 165°C and that of the s-BPDA/ODA polyimide to be about 272°C. Furthermore, DSC, TGA and DMA results revealed that thermal and mechanical properties of the blended films containing a few part per hundred (0.5-5 phr) of BSF30 were not difference from s-BPDA/ODA polyimide. Their surface characterizations were performed using Atomic force microscopy (AFM), X-ray photoelectron spectroscopic measurement (XPS), Attenuated total reflection Fourier transforms infrared (ATR-FTIR) technique, and contact angle measurements. Those techniques revealed that the surface segregation typed phase separation occurred between the two polymers. The type of substrate used in the film-casting process shows significant effect on the migration of surface segregated species with the relatively non-polar silicone-containing system enriching on the air exposed surface and vice versa. This phenomenon was revealed by ATR-FTIR spectroscopy when a relatively high BSF30 concentration was used i.e. 30 phr. Moreover, XPS disclosed that at low BSF30 concentration, siloxane segregated to the air side surface. The contact angle measurement indicated an enrichment of the hydrophobic siloxane segment in the blend films surface of the BSF30. The average water contact angle of glass side surface was 77° while that of the air side was about 102° in every blending ratio. These behaviors confirm the surface segregation phase separation in this blending pair.

Department...Chemical Engineering..... Student's signature..... 

Field of study....Chemical Engineering... Advisor's signature..... 

Academic year2005..... Co-advisor's signature..... 

ACKNOWLEDGEMENTS

This research is received partial financial support from Affair of Commission for Higher Education-CU Graduate Thesis Grant.

The author would like to express sincere gratitude to my advisor and co-advisor, Assistant Professor Dr. Sarawut Rimdusit and Associate Professor Dr. Suttichai Assabumrungrat. With their vision, intelligence, guidance, and kindness throughout the course of this research. I also would like to thank the thesis committee for their comments.

Furthermore, great appreciation is extended to all organization that had generously supported testing facilities. They are Mekttec Manufacturing Corporation (Thailand) Ltd. and Center of Excellence on Catalysis and Catalytic Reaction Engineering for the kind support in the use of thermogravimetric analyzer, UV-visible spectrophotometer and Atomic Force Microscope, and Department of Materials Science, Chulalongkorn University for the use of Contact Angle meter.

Additionally, thanks to everyone who has contributed suggestion and great help in writing up this thesis. Thanks to all my friends and everyone in the polymer engineering laboratory, Chulalongkorn University, for their discussion and friendly encouragement. I truly would like to thank everyone here. I feel so fortunate having a chance to learn here.

Finally, I would like to extend my appreciation to my parents who give their unfailing love, understanding, and generous encouragement during my studies.

TABLE OF CONTENT

	PAGE
ABSTRACT (THAI)	iv
ABSTRACT (ENGLISH)	v
ACKNOWLEDGEMENTS	vi
TABLE OF CONTENTS	vii
LIST OF FIGURES	x
LIST OF TABLES	xi
 CHAPTER	
I INTRODUCTION	1
1.1 General Introduction.....	1
1.2 Purposes of the Present Study.....	4
 II THEORY	5
2.1 Polyimide.....	5
2.1.1 Synthetic Methods: Two-step Poly(amic acid) Method.....	5
2.1.1.1 Formation of Poly(amic acid).....	8
2.1.1.2 Thermal Imidization of Poly(amic acid).....	8
2.1.2 Properties of Polyimide Films.....	9
2.1.3. Applications of Polyimide.....	11
2.2 Silicone-Containing Block Copolyimides.....	12
2.3 Factors Affecting Polymer Blend Film Morphology.....	14
2.3.1 Molecular weight of polymers.....	14
2.3.2 Composition ratio.....	14
2.3.3 Substrate surface free energy.....	15
2.3.4 Choice of solvent.....	15
2.3.5 Temperature of substrate.....	16
2.3.6 Heat treatment procedure.....	16
2.3.7 Contaminants.....	17
2.4 Surface Segregation in Polymer Blends.....	17
 III LITERATURE REVIEWS	19

IV EXPERIMENT	24
4.1 Materials.....	24
4.2 s-BPDA/ODA poly(amic acid) Preparation.....	26
4.3 Polyimide Blend Preparation and Imidization Condition.....	26
4.4 Characterization Methods.....	27
4.4.1 Attenuated Total Reflectance Fourier Transform Infrared Spectroscopy (ATR-FTIR).....	27
4.4.2 Raman Spectroscopy.....	27
4.4.3 UV-visible spectrophotometer.....	28
4.4.4 Contact Angle Measurement and Surface Tension Determination.....	28
4.4.4.1 Contact Angle Measurement.....	28
4.4.4.2 Calculation of Surface Tension (γ).....	28
4.4.5 Atomic Force Microscopy (AFM).....	30
4.4.6 X-ray Photoelectron Spectroscopy (XPS).....	30
4.4.7 Thermogravimetric Analysis (TGA)	30
4.4.8 Differential Scanning Calorimetry (DSC).....	31
4.4.9 Dynamic Mechanical Analysis (DMA).....	31
4.4.10 Mechanical Property Measurement.....	31
V RESULTS AND DISCUSSION	32
5.1 Imidization of s-BPDA/ODA Poly(amic acid) Films	32
5.2 Characterizations of s-BPDA/ODA-BSF30 Polyimide Blend Films.....	34
5.2.1 Effects of Composition Ratio on The Properties of The Blend Films.....	34
5.2.2 Effect of Cosolvent on the Phase Separation of The Blend Films.....	43
VI CONCLUSIONS	71
REFERENCES	72

	PAGE
APPENDICES	77
Appendix A Surface Characterization.....	78
Appendix B Thermal Properties Characterization.....	81
Appendix C Dynamic Mechanical Properties Characterization.....	84
Appendix D Mechanical Properties Characterization.....	85
VITA	86



สถาบันวิทยบริการ
จุฬาลงกรณ์มหาวิทยาลัย

LIST OF FIGURES

FIGURE	PAGE
2.1 Schematic representation of aromatic polyimide repeat unit.	5
2.2 Schematic of a two-step synthesis of polyimide from diamine and Dianhydride.....	7
2.3 Reaction mechanism of imide formation.....	8
2.4 Structure for polydimethylsiloxane.....	12
4.1 Chemical structures of substance used prepare polyimide and the silicone-containing polyimide used in this investigation.....	25
4.2 Synthetic scheme for the preparation of the s-BPDA/ODA poly(amic acid).....	26
4.3 Equilibrium sessile drop system; γ is the liquid-vapor, γ the solid-vapor, and γ the solid-liquid interfacial tension, respectively and θ the measured angle with respect to the surface.....	39
5.1 ATR-FTIR spectra of s-BPDA/ODA polyimide films prepared at 60°C for 8 hours, and at 150°C, 200°C, and 300°C for 1 hour at each of these temperature.....	46
5.2 RAMAN spectra of s-BPDA/ODA polyimide films prepared at 60°C for 8 hours, and at 150°C, 200°C, and 300°C for 1 hour at each of these temperature.....	47
5.3 UV-visible spectra of s-BPDA/ODA polyimide films prepared at 60°C for 8 hours, and at 150°C, 200°C, and 300°C for 1 hour at each of these temperature.....	48
5.4 TGA thermograms of s-BPDA/ODA polyimide, BSF30, and their blends as a function of BSF30 compositions.....	49
5.5 DTG thermograms of s-BPDA/ODA polyimide, BSF30, and their blends as a function of BSF30 compositions	50
5.6 DSC thermograms of s-BPDA/ODA polyimide, BSF30, and their blends as a function of BSF30 compositions.....	51
5.7 Storage moduli of s-BPDA/ODA polyimide, BSF30, and their blends as a function of BSF30 compositions.....	52

5.8 Loss moduli of s-BPDA/ODA polyimide, BSF30, and their blends as a function of BSF30 compositions	53
5.9 Loss tangent of s-BPDA/ODA polyimide, BSF30, and their blends as a function of BSF30 compositions.....	54
5.10 Contact angle measurements obtained for water drops on s-BPDA/ODA polyimide, BSF30, and their blends as a function of BSF30 compositions.....	55
5.11 Contact angle measurements obtained for ethylene glycol drops on s-BPDA/ODA polyimide, BSF30, and their blends as a function of BSF30 compositions	56
5.12 Surface tension of s-BPDA/ODA polyimide, BSF30, and their blends as a function of BSF30 compositions.....	57
5.13 ATR-FTIR spectra of s-BPDA/ODA polyimide, BSF30, and their blends as a function of BSF30 compositions on glass substrate (Air side).....	58
5.14 ATR-FTIR spectra of s-BPDA/ODA polyimide, BSF30, and their blends as a function of BSF30 compositions on glass substrate (Glass side).....	59
5.15 XPS survey scans of s-BPDA/ODA polyimide, BSF30, and their blends as a function of BSF30 compositions on glass substrate.....	60
5.16 XPS depth profiling showing Si _{2p} , S _{2p} , N _{1s} , , and C _{1s} peaks of 0.5 phr of BSF30.....	61
5.17 XPS depth profiling showing Si _{2p} , S _{2p} , N _{1s} , , and C _{1s} peaks of 5 phr of BSF30.....	62
5.18 Changes of XPS peaks of Si _{2p} of 0.5 and 5 phr of BSF30 with time of sputtering.....	63
5.19 AFM high images of s-BPDA/ODA polyimide, BSF30, and their blends as a function of BSF30 compositions.....	64
5.20 s-BPDA/ODA polyimide, BSF30, and their blends as a function of BSF30 compositions.....	65
5.21 Mechanical properties of s-BPDA/ODA polyimide, BSF30, and their blends as a function of BSF30 compositions: (■) Tensile Modulus and (●) Tensile Strength.....	66

5.22 DSC Thermograms of 3 phr s-BPDA polyimide-BSF30 blends at various cosolvent compositions.....	67
5.23 Contact angle measurements of 3 phr s-BPDA/ODA polyimide-BSF30 blends at various cosolvent compositions.....	68
5.24 AFM high images of 3 phr s-BPDA polyimide-BSF30 blends at various cosolvent compositions.....	69
5.25 UV-visible spectra of 3 phr s-BPDA polyimide-BSF30 blends at various cosolvent compositions.....	70



สถาบันวิทยบริการ
จุฬาลงกรณ์มหาวิทยาลัย

LIST OF TABLES

TABLE	PAGE
2.1 Properties of Upilex R, Upilex S and Kapton type films.....	11
4.1 Surface energy for water and Ethylene Glycol.....	29
5.1 Water contact angle of s-BPDA/ODA polyimide films prepared at 60°C for 8 hours, and at 150°C, 200°C, and 300°C for 1 hour at each of these temperature.....	45



สถาบันวิทยบริการ
จุฬาลงกรณ์มหาวิทยาลัย

CHAPTER I

INTRODUCTION

1.1 General Introduction

Since the first commercialization of polyimides in the late 1960s by Du Pont, the advancement in the science and technology of the polymers, particularly in the field of aromatic polyimides, has led to a wide range of their utilization including in the microelectronic industries as optical components or dielectric and passivation layers (Licari and Hughes, 1990; Ghosh and Mittal, 1996; and Cho et al., 2005), in membrane industries (Ghosh and Mittal, 1996 and Ohya et al., 1996) as well as in space applications (Silverman, 1995; Ghosh and Mittal, 1996; Yokota, 1999; Rimdusit and Yokota, 2002; Grossman and Gouzman, 2003; and Kiefera et al, 2003). One major space application of high performance polyimides is as multilayer metallized polymer insulations called a thermal blanket (MLI) which helps control the temperature of the instruments in the spacecraft as well as to help protect those equipment from the corrosive atomic oxygen-rich environment in low earth orbit etc. Kapton (PMDA/ODA) and Upilex R-typed (s-BPDA/ODA) polyimides respectively, are the major polyimide thermal blankets currently used in the Japanese spacecraft due to their outstanding overall mechanical, thermal, and optical properties. The powerful Japanese X-ray observatory satellite named ASCA was the first satellite to be completely covered by Upilex-R MLI (Silverman, 1995; Yokota, 1999; Kiefera et al, 2003; and Watsona et al., 2005).

Si-containing polymers such as silicone, copolymer of polydimethyl siloxane and polyimide, or polysilsesquioxane have been reported to possess high UV stability, inherent resistance to degradation in aggressive oxygen environment, enhanced solubility, impact resistance, modified surface properties, good adhesion, low stress in thin film dielectrics, fire resistance etc (Arnold et al., 1989; Furukawa et al., 1997; Tiwari et al., 2004; and Banks et al., 2002). Silicone is utilized as adhesives, sealants, or flexible parts such as in a refractive photovoltaic concentrator lenses in the

spacecraft components (Banks et al., 2002). The elastomer was reported to be a source of contaminant by-products due to its interaction with atomic oxygen to yield a denser silicon oxide film which sometimes assists in retardation of surface erosion by atomic oxygen in space. Recently, Japan Aerospace Exploration Agency (or former NASDA) had reported the AO evaluation of block copolymer of siloxane and sulfone-based polyimide namely BSF30 (NASDA Report, 2003). The materials showed superior AO resistance characteristics to other high performance polyimides such as Upilex or Apical-typed polyimide (NASDA Report, 2003 and Mochizuki et al., 1997). However, due to the incorporation of siloxane segment in the block copolymer, some properties particularly its thermal and mechanical behaviors are sacrificed (Furukawa et al., 1997 and Tiwari et al., 2004).

The utilization of polymer blends either miscible or immiscible systems by the incorporation of an oxidative resistant polymer species into the more susceptible polymers have also been investigated. One patented system of a blend of polyphenylsiloxane and Kapton-typed polyimide is already commercialized i.e. Du Pont's AOR Kapton (Tiwari et al., 2004). Since oxidative erosion is primarily a surface phenomenon, there is, in principle, no need to create an entirely new polymeric system which must be undergone thorough property evaluation prior to use. Consequently it is more practical to employ a polymer blending methodology such as of a surface segregation-typed phase separation to solve the surface oxidative erosion problems as well as to modify other essential surface characteristics of the known high performance polyimides (Mochizuki et al., 1997). This technique has major advantages over the others as it potentially provides a strong or durable coating skin layer containing minimal amount of a better oxidative resistant moieties such as siloxane, in our case, on the surface. The objective of this investigation is to identify suitable processing conditions to render a phase-separated system of a surface segregation type with the polysiloxane-block-polyimide (BSF30) on the surface of s-BPDA/ODA polyimide. The utilization of appropriate processing methods such as suitable substrates, co-solvents, or heat treatment for a polymer film formation will be explored. The phase separation behaviors of two types of polyimides, one containing silicone segments in the structure with inherent oxidation resistant property (i.e. BSF30) and another one based on well-known space durable polyimides (i.e. s-BPDA/ODA), will be investigated.

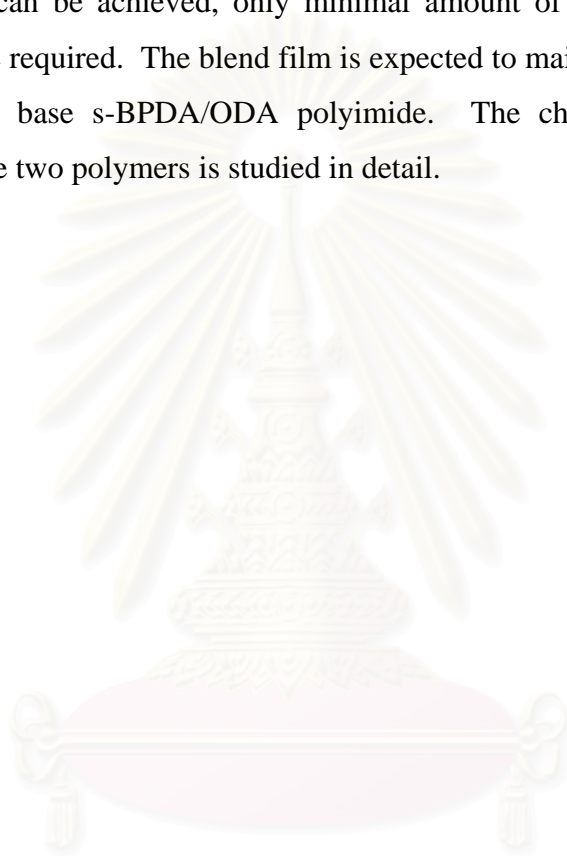
The aim of this research is to identify suitable processing conditions to render a phase separated polyimide blend systems of layer phase separation or gradient types with the silicone rich species on the surface. The methodology starts from the use of appropriate processing methods such as suitable composition and cosolvent for a polymer film formation. The surface segregation of polyimide blends result in the silicone-containing on the upper layer and the s-BPDA/ODA polyimide on the lower one. The upper surface acts as the adhesive layer, which can adhere with the other components more efficiently than s-BPDA/ODA polyimide. The advantage of this method over the others is that the film interface is stronger and even smoother. In addition, it helps reduce the production cost and steps of manufacturing process. This may be considered as the triggering point in domestic polyimide production and as the first step of processing conditions concerning the phase segregation behaviors of polyimide blends.



สถาบันวิทยบริการ
จุฬาลงกรณ์มหาวิทยาลัย

1.2 Purposes of the Present Study

The major objective of this work is to develop s-BPDA/ODA polyimide film, which potentially shows enhanced surface characteristics of adhesive property utilizing polysiloxane-block-polyimide (BSF30). If the phase separation in these blend systems can be achieved, only minimal amount of the lower thermal stable BSF30 could be required. The blend film is expected to maintain overall film thermal stability of the base s-BPDA/ODA polyimide. The characteristic of the phase separation of the two polymers is studied in detail.



สถาบันวิทยบริการ
จุฬาลงกรณ์มหาวิทยาลัย

CHAPTER II

THEORY

2.1 Polyimides

Polyimides have become one of the most important and versatile classes of high performance polymers. Due to their excellent electrical, thermal, and high temperature mechanical properties, aromatic polyimides have found many applications such as high-temperature insulators and dielectrics, coatings, adhesives, and matrices for high performance composites. The structural composition of aromatic polyimides consists primarily of heterocyclic imide and aryl groups, which are linked sequentially by simple atoms or groups, as shown in the generic repeat unit below (Figure 2.1).

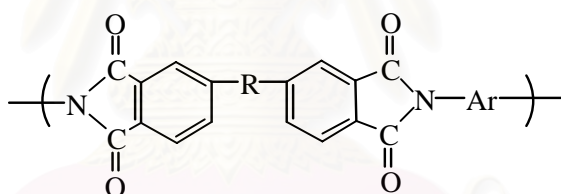


Figure 2.1: Schematic representation of aromatic polyimide repeat unit (Dunson, 2000)

Polyimides can be made by a variety of synthetic routes. Typically, the most widely used synthetic route is a two-step method. This method consists of the formation of the poly(amic acid) precursor, and the dehydration of this prepolymer to yield the final polyimide.

2.1.1 Synthetic Methods: Two-step Poly(amic acid) Method

Since the successful commercialization of Kapton by Du Pont Company in the 1960s, numerous compositions of polyimide and various new methods of synthesis have been disclosed. An accomplished result for each method depends on the nature

of the chemical components involved in the system, including monomers intermediates, solvents, the polyimide products, as well as physical conditions during the synthesis. Properties such as monomer reactivity and solubility, the glass transition temperature, T_g , crystallinity, T_m , and melt viscosity of the polyimide products ultimately determine the effectiveness of each process. Accordingly, proper selection of synthetic methods is often critical for preparation of polyimides of a given chemical composition (Ghosh and Mittal, 1996).

The two-step method for the preparation of polyimides consists of polymerization of a soluble poly(amic acid) intermediate, followed by dehydration of this prepolymer to yield the final polyimide. As illustrated in Figure 2.2, this approach is based on the reaction of a diamine with a tetracarboxylic acid dianhydride in a polar, aprotic solvent such as dimethylacetamide (DMAC), dimethylformamide (DMF), or N-methylpyrrolidone (NMP), at temperatures between 15 and 75°C (Willson, Stenzenberger, and Hergenrother, 1990). The resultant poly(amic acid) is then cyclized either thermally or chemically in a subsequent step to produce the desired polyimide.

Poly(amic acid)s are shaped into articles such as films and fibers by removing a solvent. The shaped poly(amic acid) films, for example, are thermally or chemically converted to the final polyimide products. The conversion produces water as a by-product. Because water must to be removed during this in-situ imidization, the process is generally suitable only for the preparation of thin object such as films.

When a diamine and a dianhydride are added into a dipolar aprotic solvent such as N,N-dimethylacetamide, poly(amic acid) is rapidly formed at ambient temperatures. The reaction mechanism involves the nucleophilic attack of the amino group on the carbonyl carbon of the anhydride group, followed by the opening of the anhydride ring to form amic acid group as illustrated in Figure 2.3.

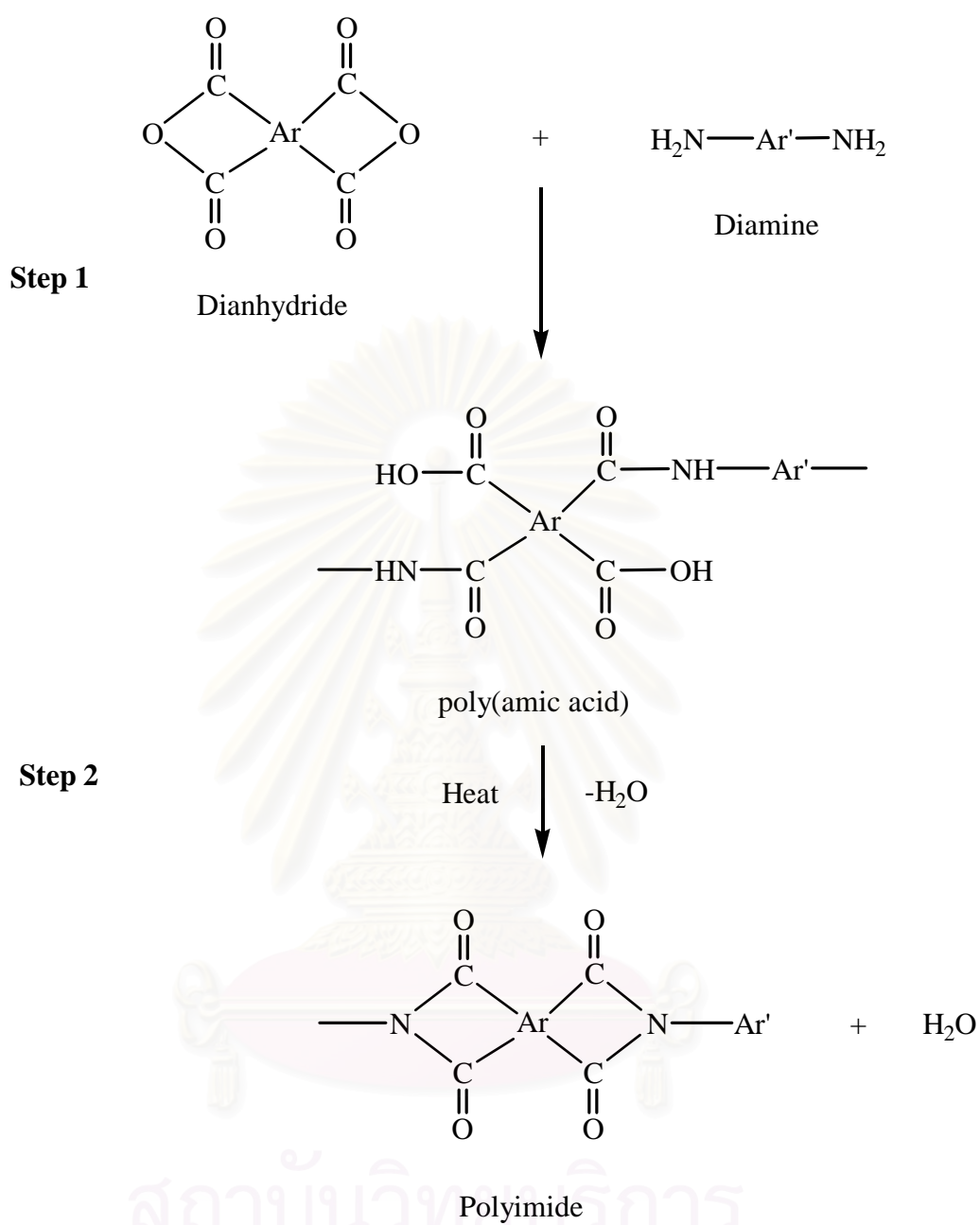


Figure 2.2: Schematic of a two-step synthesis of polyimide from diamine and dianhydride.

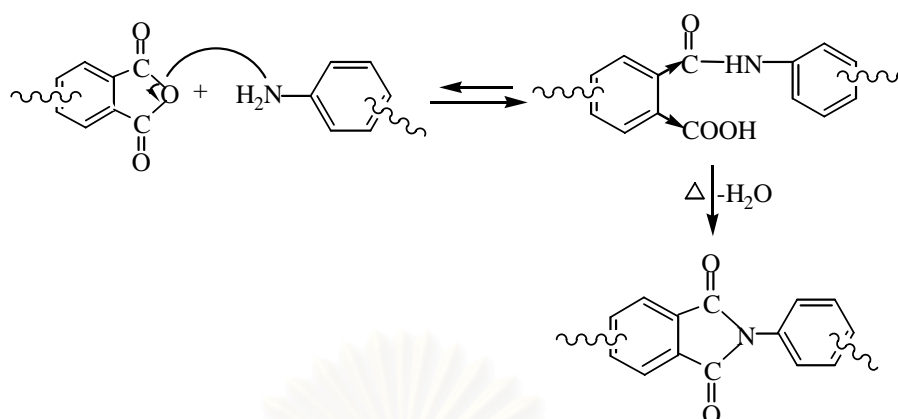


Figure 2.3: Reaction mechanism of imide formation. (Ghosh and Mittal, 1996)

2.1.1.1 Formation of Poly(amic acid)

The most important aspect of this process is that it is an equilibrium reaction. Often it appears to be an irreversible reaction because a high-molecular-weight poly(amic acid) is readily formed in most cases as long as pure reagents are used. This is because the forward reaction is much faster than the reverse reaction, usually by several orders of magnitude. If the large reaction rate difference is not met, the high-molecular-weight poly(amic acid) is not formed. Therefore, it is important to examine the driving forces that favor the forward reaction over the reverse reaction. It should also be noted that the acylation reaction of amines is an exothermic reaction and that the equilibrium is favored at lower temperatures. The forward reaction in dipolar solvents is a second-order-reaction and the reverse reaction is a first-order reaction. Therefore, the equilibrium is favored at high monomer concentrations to form higher molecular-weight poly(amic acids).

2.1.1.2 Thermal Imidization of Poly(amic acid)

Conversion of poly(amic acid)s to the corresponding polyimides is most commonly performed thermally in “solid state”. This method is suitable for preparation of thin objects such as films, coatings, fibers, and powders in order to allow the diffusion of by-product and solvent without forming brittles and voids in the

final polyimide products. The cast films are dried and heated gradually up to 250-350°C, depending upon the stability and glass transition temperature (T_g) of the polymer. Too rapid heating may cause the formation of bubbles in the sample. When a DMAc solution of poly(amic acid) is cast and dried at ambient temperature to a nontacky state, the resulting film still contains a substantial amount of the solvent (typically up to 25% by weight, depending on the drying conditions). In the subsequent heating, imidization reaction takes place not in a true solid state but rather in a very concentrated viscous solution, at least during the initial and the intermediate stages of thermal imidization. The presence of residual solvent plays an important role in the film forming behaviors. The imidization precedes faster in the presence of dipolar amide solvents. The observation is attributed to the specific solvation to allow the favorable conformation of amic acid group to cyclize. It may also be explained by the plasticizing effect of the solvent to increase the mobility of the reacting functional groups. The favorable property of amide solvent also suggests that its basicity to accept protons may be responsible for the specific effect. The proton of the carboxylic group is strongly hydrogen-bonded to the carbonyl group of the amide solvent. The cyclization of o-carboxamide group results in dehydrogen bonding and release of the solvent molecules along with water of condensation.

The most common method of converting the poly(amic acid) to the polyimide is by bulk (or melt) imidization (Bowens, 1999). Films of the poly(amic acid)s are often cast from polar aprotic solvents and subsequently dried and imidized. A typical imidization cycle may proceed by the following schedule: 100°C, 200°C, followed by 300°C. Complete cyclization is accomplished at imidization temperatures above the T_g of the material to ensure chain mobility. Imidization temperatures close to or below the T_g of the material greatly affects the % conversion of the poly(amic acid) moieties.

2.1.2 Properties of Polyimide Films

The properties of polyimides depend on many factors i.e. the starting chemicals i.e. an aromatic dianhydride, a diamine monomer, and a dipolar aprotic solvent. The conditions to produce polyimides are one of the factors, which can affect

their resulting properties as well. Polyimides have been recognized from the earliest days of their invention for their outstanding thermal stability both in air and anaerobically. These outstanding properties, in addition to thermal durability, include excellent mechanical properties from 4 to 573 K, outstanding electrical properties and stability of these electrical properties over wide range of relative humidity, intractable to solvent, and excellent radiation resistance.

This work is based on s-BPDA/ODA polyimide film, which is commercialized by Ube industries under the trade name, Upilex R. The other type, Upilex S, is the polyimide from BPDA/PPD (PPD = p-phenylenediamine), while Kapton is the polyimide film from PMDA/ODA (PMDA = pyromellitic dianhydride). The properties of Upilex R, Upilex S, and Kapton polyimide films are shown in Table 2.1.

The comparison of Kapton with Upilex R films is instructive structurally and significant in term of useful properties. Both types can be crystallized. Upilex R, carrying the same diamine as Kapton, has a significantly lower T_g (285°C versus ~385°C), but nevertheless is comparable to Kapton in mechanical and electrical properties both at room temperatures. Upilex R is superior to Kapton in having lower H₂O regain, lower 250°C shrinkage, and excellent hydrolytic resistance, particularly to aqueous NaOH.

Table 2.1: Properties of Upilex R, Upilex S and Kapton type films. (Willson et al., 1990)

Property	Upilex R (BPDA/ODA)	Upilex S (BPDA/PPD)	Kapton (PMDA/ODA)
<i>Mechanical properties</i>			
Tensile strength (MPa)	241	393	172
Tensile modulus (GPa)	3.7	8.8	3.0
Elongation (%)	130	30	70
<i>Thermal properties</i>			
Glass transition temperature, T_g (°C)	285	>500	385
<i>Chemical properties</i>			
Gas permeability			
O ₂	100	0.8	25
N ₂	30	-	6
CO ₂	115	1.2	45
He	2200	-	415
Solvent resistance	Excellent	Excellent	Excellent
<i>Electrical properties</i>			
Dielectric constant at 10 ³ Hz	3.5	3.5	3.5

2.1.3. Applications of Polyimide

Aromatic polyimide high temperature polyimides based on PMDA, BPDA, and other dianhydrides are commercially produced, mostly in the form of film. They possess high T_g and T_m and therefore the films are produced via the two-stage poly(amic acid) process. Kapton films derived from PMDA and ODA are the earliest commercial polyimides available in various thicknesses and also as surface modified

forms and others containing various inorganic fillers. Because of their outstanding thermal, mechanical, and electrical properties as well as radiation resistance, these films are widely used as insulation materials in aerospace, electric, and electric component. Another common application is flexible printed circuits made from copper-polyimide laminates. Similar high temperature films marketed as Upilex are based on BPDA and manufactured by Ube Industries. Upilex-R has high tensile strength and modulus at its used temperatures. It is also superior in hydrolytic stability. This film is widely used in many applications for example type carriers for IC chip mounting (TAB), motor coil insulation, special wires for aircraft and high-rise buildings mainframe computers and communication networks, solar cells, various types of sensor, thermal insulation for satellites, and gas separation membrane, etc.

2.2 Silicone-Containing Block Copolyimides

Linear polysiloxanes (silicone) are prepared by either polycondensation of bifunctional silanes or by ring-opening polymerization of cyclic oligosiloxanes. Linear polydimethylsiloxanes (PDMS) (Figure 2.4) are found in a wide range of commercial applications due to their excellent properties. These properties include good adhesive property, an extremely low glass temperature (-123°C), high thermal and oxidative stability, UV resistance, low surface energy and hydrophobicity, good electrical properties, high permeability to many gases, and low toxicity.

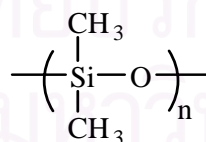


Figure 2.4: Structure for polydimethylsiloxane. (Bowens, 1999)

Silicone-containing polyimides were developed by General Electric since 1993. They come in two variations: random copolymers and block-copolymers. In random copolymers relatively low molecular weight siloxane-containing diamines are mixed with other diamines and dianhydrides in the correct stoichiometric ratio. The

chemical structure is comparable to polyisocyanates with randomly distributed hard and soft segment. In siloxane-containing block-copolyimides the hard-block is a polyimide and the soft-block is a polysiloxane. Block and graft copolymers containing relatively long siloxane units have also been synthesized (Ghosh and Mittal, 1996).

In microelectronic applications, silicone-containing polyimides are used primarily as adhesives and encapsulants. With the combined properties of the polyimide and silicone-containing polyimides copolymers have increased solubility and flexibility as compared to the polyimide homopolymer, leading to increased overall processability. The introduction of the siloxane component allows increased impact resistance, excellent adhesion, reduced water absorption, decreased dielectric constants, and increased gas permeability, while maintaining the thermal and mechanical stability that is adequate for most microelectronic applications (Furukawa et al., 1997). Silicone-containing polyimides; however, are much more complicated than the polyimide homopolymers in that there are two involved components, which have a low mixing entropy. This low mixing entropy results in microphase separation of the polymer, with a domain size that varies with block length and percentage of PDMS. Also, in copolymer systems, the low surface energy component (in this case PDMS) tends to migrate to the surface in order to minimize the total free energy of the system. Numerous studies have shown that the PDMS is likely to microphase separate and segregate to the surface in copolymer systems. PDMS has been shown to predominate in the surface of such block copolymers PS-PDMS (Chen, Gardella, and Kumler, 1993; Chen and Gardella., 1994), PMMA-PDMS (Smith et al., 1992) and nylon-6-PDMS (Polk, 2001). This phenomenon has also been shown to occur in silicone-containing polyimides copolymer systems. The extent to which this segregation occurs; however, depends on numerous variables including bulk composition, block length, processing conditions (such as annealing and casting solvent), and the block sequence distribution.

2.3. Factors Affecting Polymer Blend Film Morphology

The surface morphology of polymer blend films have become a very important subject, both experimentally and theoretically, because of their associated industrial applications such as adhesion, friction, and wetting properties, etc. To particular requirements, such as surface coatings, how to create and control films with different properties is very important. In general, phase morphology depends on polymer molecular structures, composition ratio, molecular weights, solvent selection and the method of blend preparation and can also be influenced by a suitable selection of the substrate surface free energy.

2.3.1 Molecular weight of polymers

High molecular weight induces metastable structure due to less mobility. For immiscible polymer blends, many studies on the surface morphology formation had been reported. Li, Han, and An (2003) investigated the effects of the molecular weights on the surface morphologies of PS/PMMA blend films. For the spin-coated films, three different kinds of surface morphologies (a nanophase-separated morphology, a PMMA cellular or network-like morphology whose meshes filled with PS, a sea-island like morphology) were observed when molecular weight was varied. The results indicate that the surface morphology of the polymer blend films can be controlled by the polymer molecular weight.

2.3.2 Composition ratio

In bulk materials, major component tends to form continuous phase. In thin film, interface and surface energies are important factors determining the segregation of blend components, and the component with the lower surface energy is generally enriched in the surface region in order to minimize the air-polymer interfacial free energy. Takahara and Kajiyama (1996) reported the PS/PMMA blend films, the air-polymer interfacial region was covered with a PS rich over layer due to its lower

surface free energy compared with that of PMMA and a well-defined macroscopic phase separated structure was formed in the bulk phase.

2.3.3 Substrate surface free energy

A component with the greater affinity for the substrate is more prevalent at the substrate interface. Many groups studied the effects of substrate surface free energy on the morphology. Kano et al. (1998) investigated the effect of the substrate on the gradient domain morphology for immiscible blends of poly(2-ethylhexyl acrylate-co-acrylic acid-co-vinyl acetate) [P(2EHA-AA-VAc)] and poly(vinylidene fluoride-co-hexafluoro acetone) [P(2VDF-HFA)]. They concluded that the affinity between P(2VDF-HFA) and substrate influenced the formation of the gradient domain morphology and the surface segregation of P(2EHA-AA-VAc). Walheim et al. (1997) studied the morphology formation of PS/PMMA blends onto SiO_x, Au and ODM substrate. They revealed that on the polar SiO_x and Au surface, the more polar PMMA forms a homogenous layer on the substrate. On top of this continuous layer, a characteristic phase segregated domain structure is formed. On the hydrophobic ODM surface a PS/PMMA bilayer is observed, with PS next to the substrate. The PMMA layer is punctured by holes that are partially filled by the PS-rich phase. These results showed that the substrate surface energy also played an important role. The blend surface structure was governed by the preferential orientation of one phase to the substrate. Winesett et al. (2000) observed similar features for the same system under similar condition.

2.3.4 Choice of solvent

Solvent also plays an important role in influencing the surface morphology of a polymer blend. It controls evaporation characteristics and relative solubility. Walheim et al. (1997) studied the solvent effects on the surface structure of PS/PMMA blend films. The degree of solubility and swelling of PS and PMMA in toluene, tetrahydrofuran (THF) and methyl ethyl ketone (MEK), as well as the solvent evaporation rate, controlled the final surface structure. Toluene and THF are better solvents for PS than PMMA; therefore, the PS rich phase contains more toluene or

THF than the PMMA phase. As more solvent evaporates, a characteristic time is passed where there is practically no toluene or THF left in the PMMA phase, while the other phase is still swollen with toluene or THF. Further evaporation collapses the swollen PS phase to level that lies much below the interface of the higher PMMA structures. Inversely, MEK preferentially dissolves PMMA and accumulates in the PMMA-rich phase, which leads to protruding PS domains.

2.3.5 Temperature of substrate

Temperature of substrate can affect evaporation rate of solvent and solubility of polymers. Kano et al. (1998) reported the rate of solvent evaporation as the other factor correlating the segregation towards the surface of P(2EHA-AA-VAc) because the blend film was prepared by coating from THF solution. When the rate of solvent evaporation was very fast, no segregation of P(2EHA-AA-VAc) occurred in the blend film because the polymer chains were quickly frozen before the start of the segregation towards the surface side of P(2EHA-AA-VAc). In this report, since the preparation of blend films was performed at 23°C, the rate of solvent evaporation was presumably very slow. Therefore, they presume that the segregation towards the surface side of P(2EHA-AA-VAc) was caused by the affinity between PTFE and P(VDF-HFA) and by the slow solvent evaporation rate.

2.3.6 Heat treatment procedure

Temperature above glass transition (T_g) allows significant chain mobility. Polymers are cured beyond the T_g because the molecular motion above the T_g allows tenaciously held molecules (e.g. solvent) to depart more easily and induces molecular packing. Ton-That et al. (2000) reported the effect of annealing temperature above glass transition temperature of PS/PMMA blend, the polymers behave like viscous liquids, and polymer segment movements on large scale are attainable.

2.3.7 Contaminants

Impurities can act as surfactants or compatibilizers which change phase morphology. Hayashi et al. (1998) reported the morphology of thin films casted on glass slides of a pure blend of PSU and PA. The result showed strong phase separation although the structure formation is strongly influenced by the interaction with the glass and air interface, i.e. wetting. When adding a small amount of a reactive component (a modified PSU) to the blend, the phase separation process can be suppressed completely.

2.4. Surface Segregation in Polymer Blends

Surface segregation is a phenomenon of redistribution of the components of a binary polymer blend in the solution or melt state near the interface with a solid. This effect is connected to the different thermodynamic affinity of the blend components to the surface and relates also to the disparities in the surface tension of polymer components. The phenomenon takes place when the melt or solution of polymer blends contacts with the surface. As a result, in the direction normal to the surface there arises the transition layer with the concentration gradient that determines the properties of the layer near the interface. The effect has a thermodynamic origin and is considered in the framework of modern thermodynamic theories of polymer blends.

The blending of silicones with organic polymers is of particular interest since small bulk concentrations of polydimethylsiloxane (PDMS) polymers can result in rather dramatic surface enrichment. The unique surface behavior rendered by the addition of the low surface energy PDMS component is a direct result of the structural properties of the polymer. The characteristic surface properties of PDMS are low surface tension, moderate interfacial tension against water, high water repellency (hydrophobic), no surface shear viscosity, good lubrication of plastics and elastomers, good wetting, spreading, flow-out aid, and soft feel (Owen et al., 1993).

The combined effects of the low intermolecular forces between the methyl groups and the flexibility of the siloxane backbone have been used as the basis for understanding the surface properties. From a surface tension viewpoint, the more flexible the backbone, the more readily the lowest surface energy configuration will be adopted.

Since the surface tension of PDMS is very low (≈ 20 dyne/cm) when compared to most organic polymers, the siloxane segments are expected to migrate to the more hydrophobic top (air) surface to form a silicone enriched layer. Surface energetic and molecular mobility of the PDMS component govern the surface/bulk compositional differences can be observed. This yields such properties as reduced friction, improved gloss and feel, aid in release from molds, and increased electrical properties.



สถาบันวิทยบริการ
จุฬาลงกรณ์มหาวิทยาลัย

CHAPTER III

LITERATURE REVIEWS

Many researches on synthesis and development of polyimide have been done; for example: Hergenrother et al. (2002) studied the series of new polyimides prepared from the reaction of 3,3',4,4'-biphenyltetracarboxylic dianhydride (s-BPDA) with the various aromatic diamines. s-BPDA polyimide films were cured at 250°C, 300°C, and 350°C in air tend to darken slightly in color. Near colorless films turned pale yellow while yellow films often became more intense yellow to orange. Higher curing temperatures generally improved the tensile properties at the sacrifice of color. Curing in a nitrogen atmosphere would have been desired and probably would have helped reduce color intensity of films. Hsiao and Chen (2002) investigated a series of aromatic diamines polymerized with two aromatic dianhydrides, pyromellitic dianhydride (PMDA) and 3,3',4,4'-biphenyltetracarboxylic dianhydride (s-BPDA). The resulting poly(amic acids) was thermally cyclodehydrated to yield aromatic polyimides. The polyimides were characterized by determining their glass transition temperatures (T_g). The PMDA-based (325°C) polyimides generally exhibited a higher T_g than the corresponding s-BPDA-based (270°C) analogues, but s-BPDA-based polyimides have shown much higher elongation than PMDA-based one. Currently, polyimides are widely used for advanced applications, e.g., interlayer dielectrics in thin film microelectronic packaging. Since they are based on a mature technology and satisfy the requisite properties to survive thermal, chemical, and mechanical stresses associated with microelectronic fabrication processes.

Polysiloxane-block-polyimide becomes increasingly important materials for microelectronic applications, aerospace, and printed circuit industries due to their excellent adhesive properties, low dielectric constants, distinguished properties of oxidative stability, and good overall thermal and mechanical properties (Yamada, 1998 and Andre et al., 2001). With the combined properties of the polyimide and poly(dimethylsiloxane) (PDMS) components, polysiloxane-block-polyimide can increase solubility and flexibility as compared to the polyimide homopolymer, leading

to increase overall process ability. An introduction of siloxane component offers increased impact resistance, excellent adhesion, and decreased dielectric constants (Tiwari and Nema, 2003), while maintaining the thermal and mechanical stability that is adequate for most microelectronic applications.

Yamada (1998) studied systematic thermal, mechanical, electrical, adhesive and coating properties of siloxane-modified polyimide. Based on experimental results, it can be seen that all of polyimides showed excellent thermal, mechanical, electrical, adhesive and coating properties, which are suitable for use in microelectronics coating applications. The polysiloxane block polyimides, which have the good stress relaxation properties due to their low tensile moduli, microphase separated structures possess two different glass transition temperatures. One is arising from the siloxane phase at lower temperature (T_{g1}) and the other one caused by the polyimide phase at higher temperature (T_{g2}). Polysiloxane-block-polyimides exhibited lower tensile strengths, moduli and larger elongations because the polysiloxane component incorporated into the polymer backbone. In addition, tensile modulus and strength of the polysiloxane-block-polyimides become lower.

The surface properties of poly(dimethylsiloxane) (PDMS) containing polymer blends have been investigated by several groups. Zisman et al. (1964) was the first group which reported polymer surface modification using siloxane containing copolymers, and show that the key property of PDMS is its low surface tension, which results in surface segregation of PDMS in most polymer blend systems. This property is often desirable for many applications regarding low surface energy such as antifouling coatings (Owen, 1993). Water contact angle analyses of PDMS containing block copolymer film has been used to confirm the presence of the siloxane enriched surface. This analytical technique was used to measure the yields of the relative surface tension of the material. A higher water contact angle indicated a low energy hydrophobic surface. PDMS showed a reported water contact angle of approximately 101° . Phase separated PDMS containing block copolymer films showed that water contact angle values were very close to that of pure PDMS, indicating a siloxane enriched surface. One of the key properties is its low surface energy, which results in surface segregation of siloxane at the micro- or nano-level in

most polymer blend systems. This attractive feature enables one to achieve a low energy surface when added even in small amounts to the corresponding homopolymeric system.

Furukawa et al. (1997) investigated the surface properties of the polyimide, polysiloxane-block-polyimides, and their blend. They found that the addition of 10 wt% PDMS the contact angle increased by 25° over the homopolymer. Moreover, additional incorporation of PDMS did not contribute to an increase in water contact angle. Further investigation indicated that the surface tension of the block copolymers was almost identical with that of the PDMS homopolymer. The polar component of surface tension was decreased with polysiloxane composition, while the dispersion component of surface tension was gradually increased.

Chen and Gardellar (1994) and Spanos et al. (2003) were summarized the two generic ways for modifying the surface properties of polymeric materials. The first one case called the external methods, including gas plasma treatment, plasma coating deposition, surface grafting, and photochemistry. The second method was base on, surface segregation from within the material bulk can e.g., polymer blend systems, which consisted of blending two homopolymers (A) and (B) or mixing a block copolymer (AB) with a homopolymer (A). If polymer/polymer segment (B) has a lower surface energy than that of the homopolymer/block (A), a net lowering of the surface energy of their blend system will lead to the surface enrichment of B relative to its bulk concentration. The overall driving force in this case is a net lowering of the surface energy for the polymer blend system leading to the surface enrichment of B relative to its bulk concentration. The small amounts of block copolymers behave like a surfactant and segregates to the surface region; changing the properties of this region whereas the bulk properties remain the same as the homopolymer.

Poly(dimethylsiloxane) is a low surface energy polymer ($\gamma_{\text{PDMS}} \approx 21 \text{ Dyne/cm}$) and is often found to be incompatible with other polymer systems. Therefore, PDMS can be chosen as a homopolymer or included as a segment in block copolymers for mixing into polymeric materials. Typically, this leads to surface enrichment of the

PDMS component. For instance, numerous poly(dimethylsiloxane) copolymer/homopolymer blend mixtures have been studied in the past; examples include PDMS-co-poly(methyl methacrylate)/poly(methyl methacrylate) (Inoue et al., 1990), PDMS-co-polystyrene/polystyrene (Chen and Gardella, 1998), PDMS-co-polyurethane/phenoxy (Wen et al., 1997), polycarbonate-polydimethylsiloxane block copolymer/polycarbonate (Kim et al., 2002), and polyethylene-poly(dimethylsiloxane) copolymer/polyethylene (Spanos et al., 2003)

Inoue et al. (1990) investigates the surface segregation of PDMS-co-poly(methyl methacrylate)/poly(methyl methacrylate). They reported that the polysiloxane segments of PDMS-PMMA block copolymer and their PMMA blends were accumulated on the air side surfaces of solution-cast film and surface segregation was significantly affected by siloxane chain length in block copolymers.

Consequently, blending of PDMS containing block copolymers with organic polymers can have a dramatic effect on the surface properties. Chen and Gardella (1994) investigated the surface segregation of blends prepared with PDMS block copolymers and homopolymers of polystyrene, poly(methylstyrene), and bisphenol A polycarbonate. Because of the low surface tension of the PDMS blocks, surface segregation of the PDMS blocks is found in all these AB/B blends. The authors concluded that the amount of the block copolymer in the blend, the molecular weight of the homopolymer A, and the block copolymer architecture were contributing factors that affected the surface compositions of the AB/B blends. When the PDMS was incorporated into the blends at 6% or less by weight, the surface PDMS concentrations of the blends would be as high as 95%. The PDMS surface concentrations did not change substantially when the bulk concentration the block copolymer in the blend increased from 10 to 100%.

Wen et al. (1997) studied the blend system between PDMS-co-polyurethane and phenoxy. The blend was composed of 99% by weight of phenoxy and 1% by weight of PDMS/SPU/PDMS and the films were solvent-cast onto glass substrates. It has been shown that the surface segregation of PDMS of this blends were occurred, due to PDMS low surface tension. Their results showed that at the air-polymer

interface, the Si_{2p} intensity decreases as the XPS sampling depth increases. This suggests that the Si concentration is enriched at the surface, and the Si enrichment gradually becomes less pronounced away from the interface toward the polymer bulk.

Kim et al. (2002) investigated the effects of chemical composition, block size, and casting solvent on surface properties of the modified polycarbonate were elucidated by using angle-dependent X-ray photoelectron spectroscopy (XPS) and tapping mode atomic force microscopy. XPS results showed that the siloxane segments were enriched on the surface even at bulk composition as low as 1 wt% siloxane, depending on siloxane block size and casting solvent. When the block copolymer content in the bulk was increased, a noticeable increase of the Si concentration was observed which finally reached a plateau when the bulk concentration of PDMS block was greater than about 2 wt%. The author was summarized that another key factor affecting the siloxane migration would be the solvent evaporation rate, since the solvent with higher evaporation rates imparts less time for the polymer chains to rearrange into a favorable lower energy state during film formation.

Spanos et al. (2003) studies surface segregation blend system between polyethylene-poly(dimethylsiloxane) copolymer and homopolymer of polyethylene. They revealed that the poly(dimethylsiloxane) copolymer is found to readily undergo surface segregation during annealing to produce a well-adhered polysiloxane-rich layer. On the basis of the lower surface energy PDMS segment contained in the polyethylene-co-poly(dimethylsiloxane)-co-polyethylene block copolymer ($\gamma_{\text{PDMS}} = 21$ Dyne/cm and $\gamma_{\text{PE}} = 36$ Dyne/cm), one would expect this additive to migrate toward the air-polymer interface.

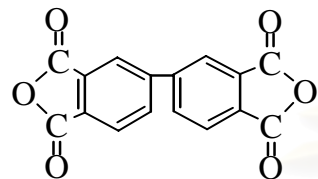
CHAPTER IV

EXPERIMENT

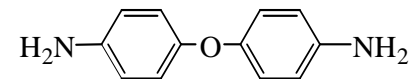
4.1 Materials

4,4'-Diaminodiphenyl Ether (ODA) was purchased from Tokyo Kasei Kogyo Co., Ltd. 3,3',4,4'-biphenyltetracarboxylic dianhydride (s-BPDA) was obtained from Ube Chemical Co., Ltd. N-methyl-2-pyrrolidinone (NMP), the solvent for poly(amic acid) synthesis, was purchased from Fluka and the cosolvent for polyimide blend, tetrahydrofuran (THF), was purchased from Merck Company. All Chemicals were used as received without any further purification. Polysiloxane-block-polyimide (BSF30) was contributed by Dr. N. Furukawa of Nippon Steel Chemical Co., Ltd. A glass petri dish was used as a substrate for polymer blend processing. The container was used after through cleaning with acetone and acid. The chemical structures of the polyimide and the copolymer use in this investigation were illustrated in Fig. 4.1.

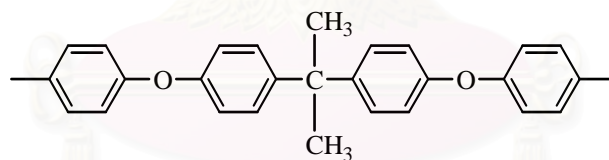
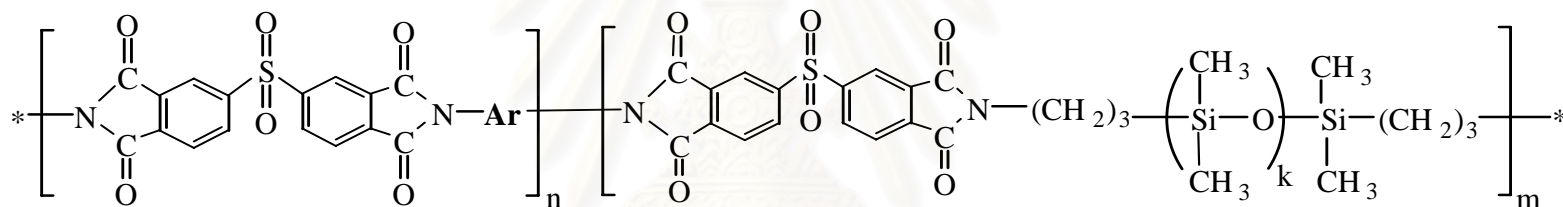
สถาบันวิทยบริการ
จุฬาลงกรณ์มหาวิทยาลัย



3,3',4,4'-biphenyltetracarboxylic dianhydride (s-BPDA)



4,4'-diaminodiphenyl ether (ODA)



Ar group

Silicone-containing polyimides (BSF30) and the corresponding Ar group

Figure 4.1: Chemical structures of substance used prepare polyimide and the silicone-containing polyimide used in this investigation.

4.2 s-BPDA/ODA poly(amic acid) Preparation

s-BPDA/ODA polyimide was synthesized by the condensation polymerization via two-step method, consisting of polymerization of a soluble poly(amic acid) intermediate. As illustrated in Fig. 4.2, this approach is based on the reaction of a diamine i.e. 4,4'-diaminodiphenylether (ODA) with a tetracarboxylic acid dianhydride i.e. 3,3',4,4'-biphenyltetracarboxylic dianhydride (s-BPDA) in a polar, aprotic, solvent such as N-methyl-2-pyrrolidinone (NMP) at room temperature. The resultant poly(amic acid) is then cyclized by thermal imidization in a subsequent step to produce the desired polyimide.

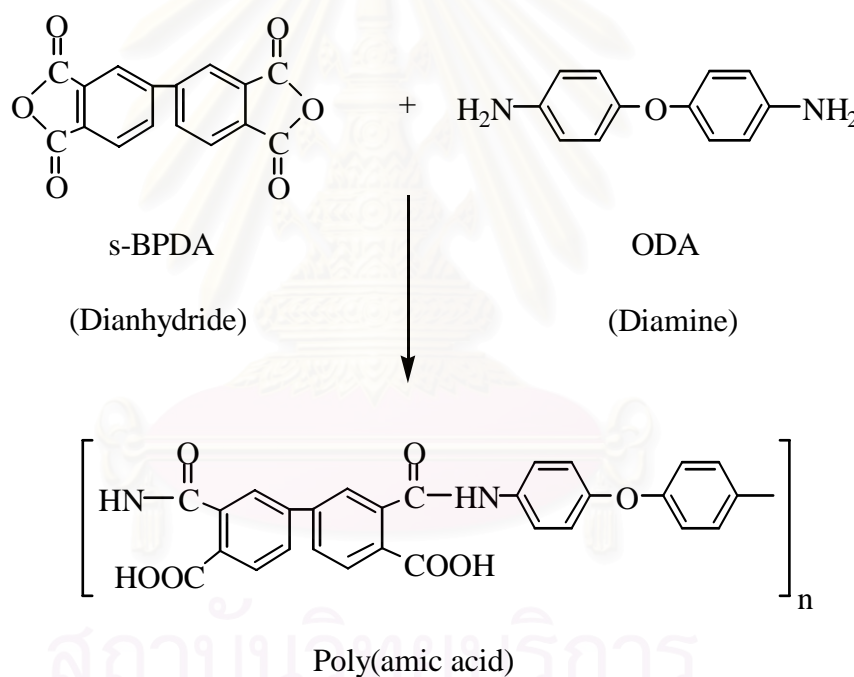


Figure 4.2: Synthetic scheme for the preparation of the s-BPDA/ODA poly(amic acid).

4.3 Polyimide Blend Preparation and Imidization Condition

Poly(amic acid) (PAA) based on s-BPDA and ODA was prepared under the conventional two-step method, whereas polysiloxane-block-polyimide solution was

made by dissolving calculated amounts of the dried copolymer film in THF solution to yield the solution having desirable concentrations. Solution mixture of the polymer blend was prepared by measuring equal mass of PAA solution and the copolymer solution and, then, thoroughly mixed using a vortex mixer. The measured amounts of the resulting clear solution mixtures were then poured onto petri dish. The mixtures were dried in an air-circulated chamber at room temperature for 3 hours and at 60°C for 8 hours. The imidization was performed stepwise using the heating program at 150°C for 1 hour, 200°C for 1 hour and at 300°C for 1 hour in a vacuum oven. Polyimide blend films obtained were cooled to room temperature and removed from the glass plates. These blend films were kept separately in sealed containers for further surface and bulk characterizations.

4.4 Characterization Methods

4.4.1 Attenuated Total Reflectance Fourier Transform Infrared Spectroscopy (ATR-FTIR)

Infrared spectrum of the air side and the glass side surface, of polyimide blend films were measured using a PerkinElmer Spectrum GX FTIR spectrophotometer. Attenuated total reflection Fourier transform infrared (ATR-FTIR) spectra were acquired using ZnSe as a prism at an incidence angle of 45°. The scan number and the spectral resolution were 64 and 8 cm⁻¹, respectively.

4.4.2 Raman Spectroscopy

FT-Raman spectra were recorded on a PerkinElmer Spectrum GX, NIR FT-Raman spectrometer equipped with a Nd/YAG laser. All samples were run over a range of 3500 cm⁻¹ to 500 cm⁻¹ using 64 scans at 8 cm⁻¹ resolution and at a power of 700 mW.

4.4.3 UV-visible spectrophotometer

The light transmission percentage through a polymer film was measured with a PerkinElmer Lambda 650 UV/VIS spectrometer. The scanned range was from 800 to 300 nm, operated at a slit beam width of 2 nm and data interval of 1 nm.

4.4.4 Contact Angle Measurement and Surface Tension Determination

4.4.4.1 Contact Angle Measurement

Contact angle measurement was performed at room temperature using a Contact Angle Meter Model CAM-PLUS MICCRO equipped with an optical microscope from TANTEC INC. The measured liquid was deionized water and ethylene glycol droplets with a radius of 10 μm . Sample's contact angle was averaged from 6-10 measured values.

4.4.4.2 Calculation of Surface Tension (γ)

The surface tension of polymer film was calculated from the obtained contact angles. As shown in Figure 4.3, their check relationship is given by Young's equation (Eq. 4.1) and Fowke's equation (Eq. 4.2) (Wu, 1982).

$$\gamma_s = \gamma_{SL} + \gamma_L \cos\theta \quad (4.1)$$

$$\gamma = \gamma^d + \gamma^p \quad (4.2)$$

Where γ_s , γ_L , γ_{SL} , θ , γ , γ^d , and γ^p are surface tensions of solid, and liquid, a surface tension between solid and liquid, a contact angle, a total surface tension, as well as dispersive and a polar components of the surface tension, respectively. The relationships between the surface tensions of solid and liquid are given by

$$\gamma_s = \gamma_s^d + \gamma_s^p \quad (4.3)$$

$$\gamma_L = \gamma_L^d + \gamma_L^p \quad (4.4)$$

$$\gamma_{SL} = \gamma_s + \gamma_L - 2(\gamma_s^d \gamma_L^d)^{1/2} + 2(\gamma_s^p \gamma_L^p)^{1/2} \quad (4.5)$$

$$(1 + \cos\theta) \gamma_L = 2(\gamma_s^d \gamma_L^d)^{1/2} + 2(\gamma_s^p \gamma_L^p)^{1/2} \quad (4.6)$$

where γ_S^p , γ_S^d , γ_L^d , γ_L^p are polar and dispersion components of surface tensions of solid and liquid, respectively. The surface tension of solid can be calculated from the data of two different liquids used in the measurement as follows:

$$(1+\cos\theta_1) \gamma_{L1} = 2(\gamma_S^d \gamma_{L1}^d)^{1/2} + 2(\gamma_S^p \gamma_{L1}^p)^{1/2} \quad (4.7)$$

$$(1+\cos\theta_2) \gamma_{L2} = 2(\gamma_S^d \gamma_{L2}^d)^{1/2} + 2(\gamma_S^p \gamma_{L2}^p)^{1/2} \quad (4.8)$$

where θ_i , γ_{Li} and γ_{Li}^p are a contact angle, a surface tension and a polar component of surface tension of liquid i ($i = 1$ or 2).

By measuring the contact angles of two different liquids with known surface energies, the surface energy of the solid can be obtained by solving Eqs. (4.7) and (4.8). Water and ethylene glycol were used and their surface energies are listed in Table 4.1.

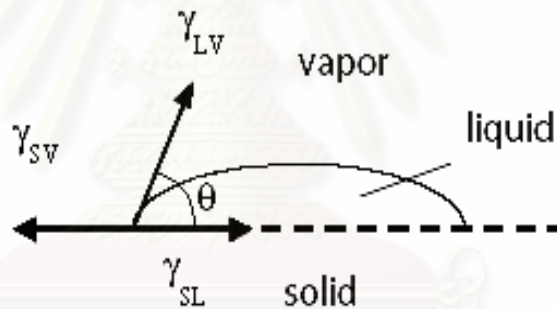


Figure 4.3: Equilibrium sessile drop system; γ_{LV} is of the liquid-vapor, γ_{SV} of the solid-vapor, and γ_{SL} is the solid-liquid interfacial tension, respectively and θ is the measured angle with respect to the surface.

Table 4.1: Surface energy for water and glycerol (Kealbe et al., 1971; Kinloch, 1987)

Liquid	γ_L^p (Dyne/cm)	γ_L^d (Dyne/cm)	γ_L (Dyne/cm)
Water	51.0	21.8	72.8
Ethylene Glycol	19.0	29.0	48.0

4.4.5 Atomic Force Microscopy (AFM)

The blend film surface topology was analyzed using an atomic force microscopy (AFM) with a NanoScope IVTM AFM (Digital Instruments, Inc.). All measurements were performed at ambient condition using a tapping mode. The etched silicon (Si) tips had spring constants of $\sim 20\text{-}1000\text{ Nm}^{-1}$ and resonance frequencies around 300 kHz. For each image, 512 lines were collected.

4.4.6 X-ray Photoelectron Spectroscopy (XPS)

A X-ray photoelectron spectrometer for depth profiling analysis is Model Escalab 220i XL from VG Scientific with a capability to analyze elements from Li to U. The low energy x-ray source was derived from the twin anode monochro x-ray gun based on Al and Mg sources. The apparatus was equipped with 6 photoelectron detectors. The analyzed area is 500 μm in diameter using the pass energy of 150 eV for the survey scan and 30 eV for the narrow scan. The machine was calibrated based on the binding energy of C_{1s} of 285.0 eV. Argon sputtering technique has been performed on blend films, where the sampling depth is defined as the surface etching with the ordinary argon sputtering. Hence, as we increase the sputtering time, we are also increasing the sampling depth.

4.4.7 Thermogravimetric Analysis (TGA)

Thermal stability i.e. degradation temperature, as well as char yield of the blend samples were evaluated using a thermogravimetric analyzer Model SII Diamond TG/DTA from PerkinElmer Instrument. The sample mass used was 5-10 mg. The heating rate was 10°C/min from room temperature to 900°C under nitrogen atmosphere. The nitrogen purge gas flow rate was 100 ml/min. Weight loss of the sample was measured as a function of time and temperature. The thermal stabilities of the polymers were reported as the 5 and 10 weight % loss temperatures.

4.4.8 Differential Scanning Calorimetry (DSC)

Thermal events and thermal transitions of polyimides and their blends were determined using a differential scanning calorimeter Model DSC 2910 from TA Instruments. The measurement was performed using a sample mass of 5-10 mg. The sample was placed in a sealed aluminum pan and was tested using a temperature ramp rate of 10°C/min from room temperature to 350°C under nitrogen atmosphere. The purge nitrogen gas flow rate was 50 ml/min. The T_g values were taken as the midpoint temperatures of the change in specific heat in the transition region.

4.4.9 Dynamic Mechanical Analysis (DMA)

Dynamic mechanical properties of the polyimide blend systems were tested using the NETZSCH Model DMA 242. The experiment is done in a tension mode using the dimension of the specimen of approximately 23.7×5×0.02 mm³ (L×W×T). The applied strain amplitude was 0.3% at the deformation frequency of 1 Hz. The specimen was heated using a temperature ramp rate of 3°C/min from room temperature to 350°C.

4.4.10 Mechanical Property Measurement

Tensile modulus and tensile strength of polyimide blend films were determined utilizing a universal testing machine (model 5567) from Instron Instrument. The test method used was a tension mode with a specimen dimension of 8.0 cm in length, 0.50 cm in width, and 0.022–0.026 mm in thickness. The specimen gauge length was 4.0 cm and the crosshead speed for film testing was 0.50 cm/min. The tensile properties were obtained following the general procedure in ASTM D882 using four to five specimens per test condition.

CHAPTER V

RESULTS AND DISCUSSION

5.1 Imidization of s-BPDA/ODA Poly(amic acid) Films

Polyimide film based on s-BPDA/ODA was prepared by casting its poly(amic acid) solution on a glass substrate followed by thermal treatment at 60°C for 8 hours, and 150°C, 200°C, and 300°C for 1 hour at each of these temperatures. Contact angles of the polyimide films for an air side and glass side were measured by one liquid method. Table 5.1 shows water contact angles of the poly(amic acid) to increase with an increase of imidization temperatures of both glass-contacted surface and air-exposed surface. The phenomenon implied that the surface of the polyimide films of both air and glass sides became less polar with the thermal imidization. The decrease of polar component of the contact angle can be interpreted based on the fact that polar functional groups of the poly(amic acid) such as carboxylic acid and amide groups were transformed into the less polar imide groups with the progress of the imidization reaction. Moreover, the contact angle of the polyimide film on the air-exposed surface was found to be greater than that of the glass-contacted surface especially with the increase of the level of imidization reaction. This was due to the hydrogen bonding between silanol groups on glass surface and the carboxylic acid and amide groups on the polyimide film surface preventing fully dehydration reaction of poly(amic acid) to polyimide on the glass side surface to be fully achieved. This result is in good agreement with those reported by Zuo et al. (1998).

Fig. 5.1 shows the IR spectra for monitoring the advancement of the polymerization of poly(amic acid). From the figure, the characteristic peaks for the poly(amic acid) at 1710 cm^{-1} for carboxylic acid group (COOH), at 1660 cm^{-1} for carbonyl group (C=O) in CONH, and at 1540 cm^{-1} for C-NH stretch band, were present at 60°C heat treatment. With increasing the treatment temperature above 150°C, the s-BPDA/ODA polyimide ring-closing reaction led to a chain growth as indicated by the disappearance of the above characteristic poly(amic acid) bands. An identification of the polyimide formation was performed by observing the imide

bands at 1775 cm^{-1} for symmetrical carbonyl stretching vibrations, at 1710 cm^{-1} for asymmetrical carbonyl stretching vibrations, at 1370 cm^{-1} for stretching vibrations of C-N, and at 738 cm^{-1} for cyclic carbonyl bending vibrations. These absorption bands were observed after heating to 150°C and higher indicating the onset of the imidization reaction to be at about 150°C . Complete imidization was achieved after heating at 200°C for 1 hour. This thermal treatment step caused the formation of carbonyl group as indicated by the appearance of its absorbance band at 1710 cm^{-1} , which overlapped with the carboxylic acid of poly(amic acid) at the same wavenumber. Subsequent heating at 300°C for 1 hour; however, did not result in any significantly additional changes in the IR spectra. This result is also consistent with those reported by Gardner (1998), Nah et al. (2004), and Yang and Su (2005).

FT-Raman analysis was carried out for specimens treated with a set of thermal imidization steps to monitor the thermal imidization processing detail. The obtained spectra are shown in Fig. 5.2. The Raman peaks at 1330 cm^{-1} corresponding to C-N stretch of the amide group, were observed for poly(amic acid). This peak became smaller with the continued thermal treatment and no detectable peaks were observed after thermal imidization step at 150°C . The ring-closing reaction to form the polyimide can be monitored by the disappearance of the C-N stretch of the amide group at 1330 cm^{-1} , and by the appearance of those bands associated with the imide moieties at 150°C and higher temperatures including imide I (1775 cm^{-1}), imide II (1380 cm^{-1}), and imide III (1110 cm^{-1}). This implied that thermal imidization began at the temperature of 150°C , and continued with further increasing in the thermal imidization temperature. This result is also consistent with those reported by Konieczny et al., (1997), Nah et al. (2004).

Fig. 5.3 illustrates an effect of treatment temperature on UV-visible transmission spectra of s-BPDA/ODA polyimide film casted on a glass substrate. The treatment temperatures were 60°C for 8 hours and at 150°C , 200°C , and 300°C for 1 hour at each of these temperatures. The optical transparency or percentage of light transmission through the film at a wavelength of 500 nm was determined for each film. Light transmission of the s-BPDA/ODA polyimide film was found to decrease as the treatment temperature of the film increased. The percentage of light

transmission for s-BPDA/ODA polyimide films at those treatment temperatures was approximately 85% for 60°C treated film, and decreased to 73% for the 300°C treated film. This was in good agreement with our visual observation that the films became systematically more yellow with increasing the treatment temperature, i.e. the films showed near colorless, pale yellow, light yellow, and yellow with the treatment temperatures.

Color in polyimide films could be caused by several factors such as chromophoric groups, impurities in the monomers or solvents, isoimide formation, charge transfer complexes, and oxidation during the curing (drying) process. Charge transfer complexes have long been associated with color in polyimide films and those factors, that can lower the charge transfer complex (CTC), will contribute to less color in polyimide films (Hergenrother et al., 2002). Raising the treatment temperature of the s-BPDA/ODA polyimide to 150°C, 200°C, and 300°C; therefore, lead to the increase of the charge transfer complex and interaction between the polymer chains. The result is also in good agreement with those reported by Hergenrother et al. (2002), who studied the a-BPDA/1,3,3-APB polyimide film. They reported that the light transmission decreased as the cure temperature of the film increased.

5.2 Characterizations of s-BPDA/ODA-BSF30 Polyimide Blend Films

5.2.1 Effects of composition ratios on the properties of the blend films

Thermal stability of polysiloxane-block-polyimide (BSF30), s-BPDA/ODA polyimide, and their blends is shown in Fig. 5.4 and 5.5. Though BSF30 was reported to show outstanding oxidative degradation as well as good adhesion, its thermal stability is clearly inferior to typical aromatic non-silicone containing polyimides such as s-BPDA/ODA as seen in Fig. 5.4. From the TGA thermogram, it was seen that BSF30 exhibited a 5% weight loss at 430°C and a 10% weight loss was about 452°C whereas those of s-BPDA/ODA showed the values of 572°C and 590°C respectively. Char yield of the BSF30 reported at 800°C was only 31% by weight, while that of s-BPDA/ODA was approximately 60% by weight. The value was almost twice the

value of the silicone-containing block copolymer. In this work, it was our major goal to develop a polyimide film which showed a surface characteristics of the BSF30 while maintaining the outstanding thermal properties of the base s-BPDA/ODA. The surface segregation-typed phase separation of the two polymers was thus purposely induced. From the thermal stability of the two polymers, if the surface segregation phase separation was achieved in these blend systems, only minimal amounts of the BSF30 would be required in order to maintain the overall film thermal stability with the desirable surface properties.

In Fig. 5.4, the blend compositions ranging from 0.5 to 30 phr of BSF30 in s-BPDA/ODA were examined. It was clearly seen that when relatively large amount of BSF30, i.e. 30 phr, was in the blend film, the thermal stability of the film would substantially be sacrificed. From the DTG thermograms in Fig. 5.5, at high composition of BSF30 in the blends i.e. 30 phr, the degradation temperature showed two dominant peaks at 425°C and 610°C which belonged to the BSF30 and the s-BPDA/ODA polyimide respectively. From this result, it can be concluded that s-BPDA/ODA polyimide and BSF30 are immiscible in nature and the phase separation was occurred giving the characteristic degradation peaks of each polymer in the blend films. On the other hand, no significant change in degradation temperature was observed in the composition range of 0.5 to 5 phr of the blend systems.

DSC thermograms of the polyimides and their blends are exhibited in Fig. 5.6. This figure also revealed the phase separation of the two polymers with the two distinct T_g s detected when the BSF30 contents were sufficiently high e.g. 30 phr. From the DSC thermograms, the glass transition temperature (T_g) of the s-BPDA/ODA polyimide and polysiloxane-block-polyimide (BSF30) were determined to be 272°C and 165°C, respectively. At relatively small amounts of the BSF30 in the blends, ranging from 0.5 phr to 5 phr, only single dominant T_g in these thermograms was observed at about 270°C; however, the thermal transition was clearly observed when the BSF30 content was raised to 30 phr. The first T_g appeared in the lower temperature range of about 166°C belonged to the BSF30 fraction. The second T_g situated at higher temperature of about 270°C was obviously the

characteristic thermal transition of the s-BPDA/ODA polyimide fraction. This behavior also confirmed the immiscibility of these blend systems and the two domains clearly exhibited their own thermal characteristics. The behaviors confirmed those results in the TGA experiments of the previous section.

Fig. 5.7 illustrates storage moduli of the s-BPDA/ODA polyimide, the BSF30, and their blends. The thermograms revealed the glassy state moduli, reported at 30°C, of the s-BPDA/ODA film to be approximately 2.86 GPa and that of BSF30 to be 1.47 GPa. The BSF30 is, therefore, much less stiff than the s-BPDA/ODA due to the presence of the soft silicone segments in its molecular structure. Thermal stability of the polymers can be seen from the slope of the glassy state moduli in the DMA thermograms. The lower the slope of the glassy state modulus, the greater thermal stability of the polymer. As a result, the DMA thermograms implied that the s-BPDA/ODA was significantly more stable than the BSF30.

The large decrease in the storage moduli at elevated temperature, about one order of magnitude in our case, indicated the beginning of the corresponding glass transition region of each specimen. The storage moduli of the blend films especially at a large BSF30 content of 30 phr clearly showed the mixed characteristics of the two parent polyimides. The blend film displayed two successive drops in its storage moduli, one starting at about 160°C and another one starting at 260°C. The value corresponded to those thermal transitions of BSF30 and s-BPDA/ODA systems, respectively. However, when the amount of the BSF30 in the blend films was kept to be in the range of few parts per hundred, i.e. 0.5 to 5 phr, the decrease of their storage moduli at about 160°C due to the presence of BSF30 was suppressed and hardly detected. In addition, the rubbery plateau modulus of the BSF30 was found to be significantly lower than those of the s-BPDA/ODA polyimide. The tighter molecular packing with greater intermolecular interaction of the s-BPDA/ODA might be one reason of these mechanical behaviors. The resulting thermograms, again, emphasized the requirement of using a relatively small amount of the BSF30 in the blend systems in order to maintain the overall thermal and mechanical integrity of the blend films.

Fig. 5.8 illustrates the loss moduli of the polyimide films in the temperature range of 30-350°C. A peak of a loss modulus was assigned as a glass transition temperature, T_g , of each specimen. In the case of BSF30, we could observe a loss modulus peak at about 158°C whereas that of s-BPDA/ODA polyimide was about 290°C. The obtained dynamic mechanical properties of the BSF30 were also similar to the systems previously reported by Furukawa et al. (1997) based on the same content of the silicone fraction. Furthermore, the loss moduli of the blend systems with BSF30 content of 30 phr showed two distinct T_g s centered around 160°C and 290°C which were the T_g s of the BSF30 and s-BPDA/ODA polyimide, respectively. The appearance of the two T_g s in our polyimide blends corresponding to the T_g of each species implied immiscibility of the polymer pair. Therefore, s-BPDA/ODA and BSF30 unavoidably underwent phase separation upon the film forming process.

Moreover, $\tan\delta$ of the polyimides and their blends is depicted in Fig. 5.9. The magnitude of $\tan\delta$ peak generally reflects the large scale mobility associated with α relaxation process whereas the width of the $\tan\delta$ relates to the homogeneity of the materials. The $\tan\delta$ peak at lower temperature of 180°C could be attributed to that of the BSF30 domain and the peak at higher temperature of 296°C was attributed to that of the s-BPDA/ODA polyimide phase. The two peaks could be observed in the blend systems, again, when sufficiently large content of the BSF30 minor phase was presented such as at 30 phr, confirming the immiscibility of the blends.

From the above results, the s-BPDA/ODA polyimide and BSF30 blends exhibited a two phase morphology; therefore, the glass transition temperatures of both components could be observed. The lower T_g corresponds to the glass transition temperature of the BSF30 phase (~160°C). The higher T_g corresponds to the glass transition temperature of s-BPDA/ODA polyimide phase (~280°C). Both values were similar to those reported elsewhere (Yamada, 1998; Tiwari et al., 2004). Although, the results from TGA, DSC, and DMA clearly indicated the immiscibility in these polyimide blends, these techniques could not predict what type of phase separation occurred in our blends. Phase separation of polymer blends containing one minor and one major phase can be roughly classified into a sea-island type and a surface-

segregated type. These two types of phase separations can be analyzed using a contact angle measurement. The sea-island type will follow Cassie's equation, while the surface-segregated type will not (Cassie, 1948).

In general, high water contact angle is indicative of a hydrophobic low energy surface. Fig. 5.10 shows a change in water contact angles of the s-BPDA/ODA polyimide and BSF30 blend films, casted on a glass substrate, as a function of the BSF30 content. From the experiment, the water contact angles of the neat s-BPDA/ODA polyimide film on the air-exposed surface and on the glass-contacted surface were measured to be 82° and 78° whereas those of the BSF30 film were 106° , and 96° . Interestingly, the water contact angles of all blend films on the air-exposed surface were about the same as the values of 102° and those of the glass-contacted surface were averaged to be 77° . The contact angles of all blend films on the air-exposed surface were found to be almost constant at 101° - 102° even at the presence of only small amount of the BSF30 (i.e. 0.5 phr). Further incorporation of BSF30 into s-BPDA/ODA polyimide would not contribute to the increase in water contact angle beyond this value. The values reaching 102° for these polyimide blends were comparable to the water contact angle on the air side of the neat BSF30 itself. In the literatures, polydimethylsiloxane (PDMS) was reported to possess an average water contact angle value of approximately 101° - 103° (Owen, 1993; Bowens, 1999). This implied that on the surface of the BSF30 and of the blends containing BSF30, siloxane species tended to migrate to the air-exposed surface, thus giving the contact angle approaching that of siloxane moieties.

The above results indicated that surface segregation occurred in s-BPDA/ODA polyimide and BSF30 blend films. Surface segregation of this blend films on the air-exposed surface provided the water contact angle very close to that of pure PDMS. The glass side surface, on the other hand, was enriched with s-BPDA/ODA polyimide fraction thus showed smaller value of water contact angle of 77° which is the signature value of that on the glass-contacted surface of s-BPDA/ODA polyimide species. The s-BPDA/ODA polyimide is more hydrophilic than the BSF30 thus tends to migrate to the more polar glass substrate to yield this surface segregation phase separation. The water contact angle of the glass-contacted side showed almost

constant value of about 77° for all tested blend compositions. Fig. 5.11 exhibits the similar results on the change in contact angles based on ethylene glycol droplets. The increase of the contact angle values was also observed even at a small BSF30 fraction in blends although the values were smaller than the contact angles against water.

The surface tension and its polar and dispersion components of the blend films were calculated by putting the contact angle data into Eq. (4.7) and (4.8). The results were plotted against the BSF30 composition in Fig. 5.12 for the air side surface. It was obvious that the polar component of the surface tension decreased with increasing the BSF30 composition while the dispersion component showed an opposite trend. The sum of both components, which is the surface tension of the film, was the lowest at the presence of the BSF30 even at the content as low as 0.5 phr in the blends. The low value of 22 dyne/cm is almost identical with the literature surface tension value of PDMS (21.8 dyne/cm) (Owen, 1993). Therefore, the air-exposed surface of the blend films was believed to be covered with polysiloxane segments of the BSF30 block copolymer. This result is consistent with those reported by Furukawa et al. on the surface characteristics of the poly(imide siloxane) block copolymer (Furukawa et al., 1997). Therefore, the polysiloxane moieties in BSF30 are expected to migrate to the air-exposed surface of the blend films to form a silicone-enriched layer.

Attenuated total reflectance Fourier transform infrared (ATR-FTIR) technique was used to confirm above surface segregation phase separation characteristics of these blend systems. This technique could also be used to explore molecular species on the surface through their vibration states and to provide an information on chemical bonds as well as molecular orientation. Fig. 5.13 and 5.14 showed the systems of the s-BPDA/ODA polyimide blended with 0.5 to 5 phr, and 30 phr of BSF30. At the blend containing 30 phr of the BSF30 in Fig. 5.13, the absorption bands at 1060 cm^{-1} , and 1015 cm^{-1} , which represented the Si-O-Si stretching vibrations and at 795 cm^{-1} of Si-C stretching were detected. They are important vibrational signatures of siloxane group in the BSF30. These peaks appeared in the air-exposed surface but were absent in the glass-contacted surface of the blend films (Fig. 5.14). Nevertheless, for lower BSF30 composition (0.5-5 phr), those three signature bands of the siloxane were not detected on the air-exposed surface (i.e. at

1060 cm^{-1} , 1015 cm^{-1} and 795 cm^{-1}). As a consequence, at very diluted blend compositions (i.e. 0.5-5 phr) which yield a submicron layer of the BSF30 domain, the technique is not sensitive enough to acquire those siloxane vibrations on the surface. This is due to the fact that ATR-FTIR technique is sensitive to the chemical species with sufficient depth depending on the type of the crystal used. In our case, a ZnSe crystal used will provide a depth profile in the range of 2-4 μm . Due to the insufficient sensitivity of ATR-FTIR to obtain an information on a very thin layer on the blend surface, X-ray photoelectron spectroscopy (XPS) was also utilized.

X-ray photoelectron spectroscopy measurements were used to further verify surface segregation in BSF30 and s-BPDA/ODA polyimide blend films especially in the low concentration range of the BSF30. Fig. 5.15 illustrated the survey scans of 0.5, 1, 3 and 5 phr blend films. The investigation was performed on both glass side and air side surfaces. As apparent from the spectra, no detectable signal of silicon was observed on the glass side film surface. However, on the air side surface the peaks due to Si_{2p} , S_{2p} , O_{1s} , N_{1s} , and C_{1s} were detected at 101-95, 168-162, 533-523, 400-393, and 290-276 eV, respectively. The Si_{2p} signal is evidently associated with the siloxane moieties in the BSF30. The obtained spectra; therefore, reflected the surface migration of the siloxane species to the air-exposed surface while the more hydrophilic molecules of s-BPDA/ODA polyimide tended to remain close to the glass-contacted surface. As the surface energy of siloxane is very low compared to that of the polyimide, the siloxane segments are expected to migrate to the more hydrophobic air-exposed surface as observed in our blends. The surface segregation of our blend films even at a small content of the BSF30 was; therefore, achieved.

Depth profile of the silicone moiety on the air-exposed surface of the blend films was also studied. In the examination, the polyimide blend film was subjected to the surface etching with an argon sputtering technique. Narrow scans were conducted on the elements obtained in the survey scans at their characteristic binding energies. Fig. 5.16 shows changes of the XPS peaks with sputtering time of the 0.5 phr blends films. It was noted that most of the S_{2p} peak detected at 165 eV shifted to 160 eV. The phenomenon was observed previously by Furukawa (1997) as a result of bond

breakage of the sulfone group by the argon sputtering. The intensity of the Si_{2p} peak also decreased with increasing sputtering time. According to Fig. 5.16, the Si concentration showed gradient structure with depth of the film with the highest concentration on the top most of the air-exposed surface. Thereafter, the Si concentration gradually decreased with sputtering time in an exponential decay manner. Further studies of XPS depth profiling revealed that increasing the BSF30 composition actually resulted in an increase in the thickness of the silicone-rich top layer. Fig. 5.17 depicts the peak changes as a function of sputtering time on the air side surface of the 5 phr blend film. It can be seen that the result exhibited the same trend of the depth profile of the Si_{2p} atom as observed in the 0.5 phr blend film. The siloxane profiles on the blend films of the 0.5 and 5 phr of the BSF30 as a function of sputtering time were also compared in Fig. 5.18. From this figure, it can be concluded that at 5 phr of BSF30, the silicone-containing layer was thicker than that of the 0.5 phr blend film over the whole sputtering time of 180 seconds.

Surface morphology of the solvent-casted s-BPDA/ODA polyimide, BSF30, and their blend films, was characterized with tapping mode atomic force microscopy. The images of the surface topography obtained from the blend films are shown in Fig. 5.19. It was noted that the surface of the s-BPDA/ODA polyimide film was relatively flat and smooth while all the blend films (i.e. 0.5, 1, 3, and 5 phr) showed rougher surface than the neat s-BPDA/ODA film. The surface roughness should be related to the surface segregation of the siloxane domains of the BSF30 on the base s-BPDA/ODA polyimide film as described in the previous sections. The domains on the 0.5 to 5 phr blend surfaces attributed to those of the siloxane that migrated to the air-exposed surface due to the low surface tension of the siloxane. In this experiment, the surface roughness of the blend films at the low contents of BSF30 (i.e. 0.5, 1, 3, and 5 phr) was observed to be highly alike in appearance. The similar topography of all blend films was; therefore, consistent with the contact angle measurement that is the water contact angles were close to that of siloxane species and did not change with the BSF30 composition, in the investigated composition range. At a greater content of the BSF30 (i.e. 30 phr), the surface topography was found to be very rough and could be observed visually.

Fig. 5.20 shows the macroscopic images of the s-BPDA/ODA polyimide, BSF30, and their blend films at various composition of BSF30. It could be seen that s-BPDA/ODA polyimide and the blend film were transparent and became slightly translucent with increasing the BSF30 content due to the phase separation of the two polymers. The films maintained their degree of transparency relatively well even at the BSF30 content up to 30 phr. No obvious change in the film transparency was observed in those films with few parts per hundred of the BSF30 fraction.

In the next section, mechanical integrity of the blend films was also evaluated. The blends of the s-BPDA/ODA poly(amic acid) and the BSF30 precursor were cast onto a glass substrate and imidized using the staged thermal imidization cycle used in the previous experiment. The films were stripped from the glass substrate and tested for mechanical properties. The values of mechanical properties of the s-BPDA/ODA polyimide and BSF30 blend films are illustrated in Fig 5.21. From the table, the tensile modulus of neat s-BPDA/ODA polyimide film was determined to be about of 2.64 GPa, and the tensile strength was 138 MPa. These values are in good agreement with those reported elsewhere (Willson et al., 1990). The increase of BSF30 fraction in the range of 0.5 to 5 phr did not significantly affect the tensile modulus of the blend films; however, further increase in the BSF30 content to 30 phr caused the decreased in the tensile modulus of the blend specimen to 1.43 GPa with the lower tensile strength of 65 MPa. From this behavior, it can be concluded that, tensile modulus and tensile strength of the blend films at the high BSF30 content such as 30 phr tended to decrease with increasing the BSF30 mass fraction in the polymer blends, while the tensile properties of the blend films with the low content had no significant change from that of pristine s-BPDA/ODA polyimide. The major aim of this study is to modify surface characteristics of a polyimide film such as to enhance the surface adhesion and to maintain its outstanding mechanical properties by attempting to fabricate the phase separation of surface segregation type of the two polymers. In order to achieve this goal, the content of the softer BSF30 component; therefore, should not exceed the few parts per hundred compositional ranges.

5.2.2 Effect of cosolvent on the phase separation of the blend films

From our experiment, the effect of cosolvent, i.e. THF on solution mixtures of BSF30 and poly(amic acid) of s-BPDA/ODA in NMP was also examined. In this investigation, the solution mixtures of s-BPDA/ODA poly(amic acid) in NMP and of dried BSF30 were prepared to yield a blend composition of 3 phr. THF cosolvent was then added. The resulting mixtures were found to be homogenous when THF/NMP was less than 150% (w/w), whereas heterogeneous solution was rendered at a higher percentage of the THF. This is because the BSF30 showed good solubility in THF while the s-BPDA/ODA polyimide did not. Excessive amount of THF (i.e. > 150% (w/w)) can, thus, result in the phase separation of the solution.

DSC thermograms in Fig. 5.22 reveal glass transition temperature (T_g) of the s-BPDA/ODA polyimide and the BSF30 blends at different cosolvent contents. Those specimens showed single T_g at 266°C, 267°C, 268°C, and 268°C for 0, 50, 100, and 150 % (w/w) of THF/NMP, respectively. The DSC thermograms revealed that the amount of the cosolvent did not significantly affect glass transition temperatures of these blend systems.

The effect of the amount of the cosolvent on the water contact angles of the polyimide blend films is also shown in Fig. 5.23. The water contact angles of the blend films at various amounts of the THF were relatively constant with the values of 102° and 77° for the air-exposed surface and the glass-contacted surface, respectively. The results again suggested that the amount of the cosolvent showed negligible effect on the surface properties of blend films. It was also in good agreement with the AFM topography shown in Fig. 5.24. The surface morphology of the 3 phr BSF30 polyimide blends at different cosolvent contents was observed to show no major difference from each other. From this result, it was concluded that the cosolvent composition did not play a role in altering the surface morphology of polyimide blend films.

Fig. 5.25 illustrates the UV-visible spectra of the polyimide blend films casted with various cosolvent compositions. It can be seen that the percentage light

transmission of the polyimide films was also not significantly different from each other. Consequently, it can be concluded that the cosolvent composition showed no major effect on the phase separation of these blend films. The only major function of the cosolvent was to improve the processing characteristics of the polymer blends by decreasing the viscosity of the blend solution.



สถาบันวิทยบริการ
จุฬาลงกรณ์มหาวิทยาลัย

Table 5.1: Water contact angle of s-BPDA/ODA polyimide films prepared at 60°C for 8 hours and at 100°C, 150°C, 200°C, and 300°C for 1 hour at these temperatures.

Side	Contact Angle (Degree) at			
	60°C	150°C	200°C	300°C
Air	69	77	80	83
Glass	64	69	72	77

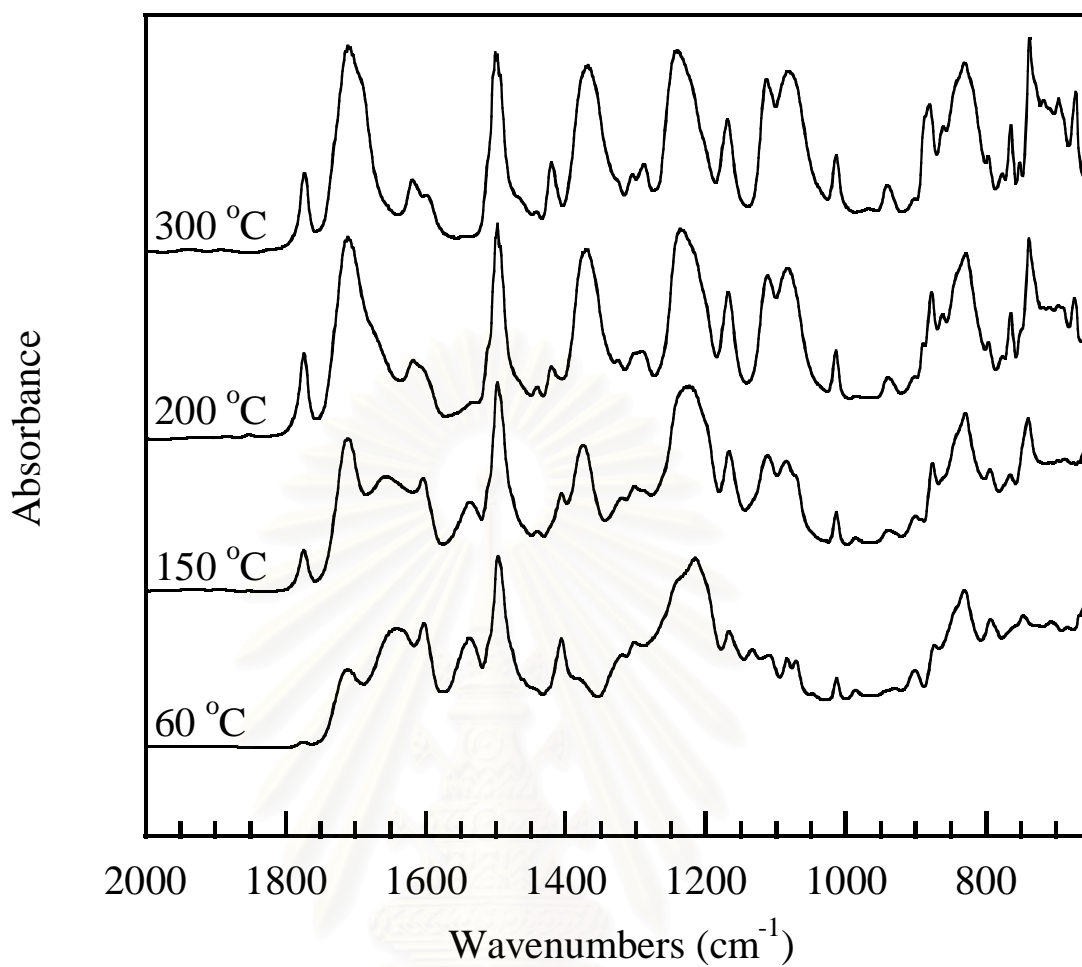


Figure 5.1: ATR-FTIR spectra of s-BPDA/ODA polyimide films prepared at 60°C for 8 hours and at 150°C, 200°C, and 300°C for 1 hour at each of these temperatures.

สถาบันวิทยบริการ
จุฬาลงกรณ์มหาวิทยาลัย

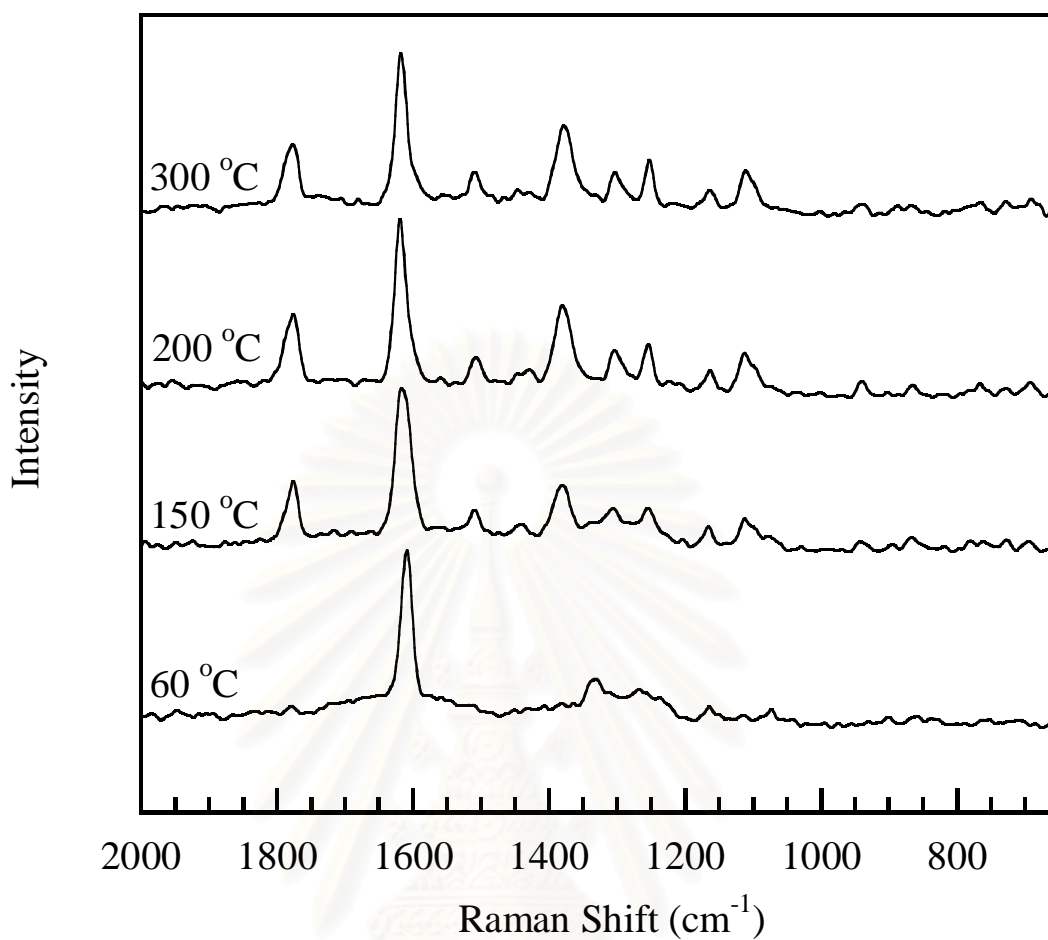


Figure 5.2: RAMAN spectra of s-BPDA/ODA polyimide films prepared at 60°C for 8 hours and at 150°C, 200°C, and 300°C for 1 hour at each of these temperatures.

สถาบันวิทยบริการ
จุฬาลงกรณ์มหาวิทยาลัย

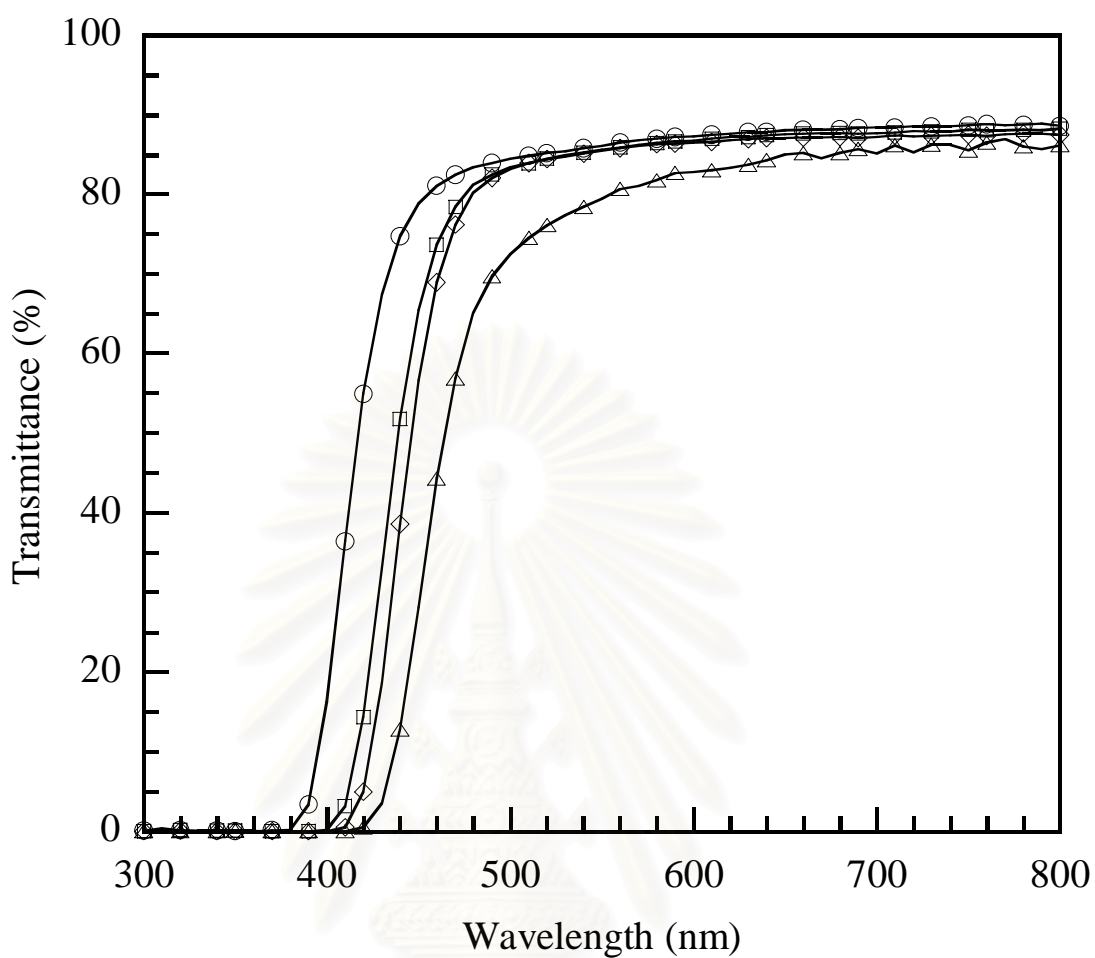


Figure 5.3: UV-visible spectra of s-BPDA/ODA polyimide film prepared at 60°C for 8 hours and at 150°C, 200°C, and 300°C for 1 hour at each of these temperatures: (○) 60°C, (□) 150°C, (◇) 200°C, (△) 300°C.

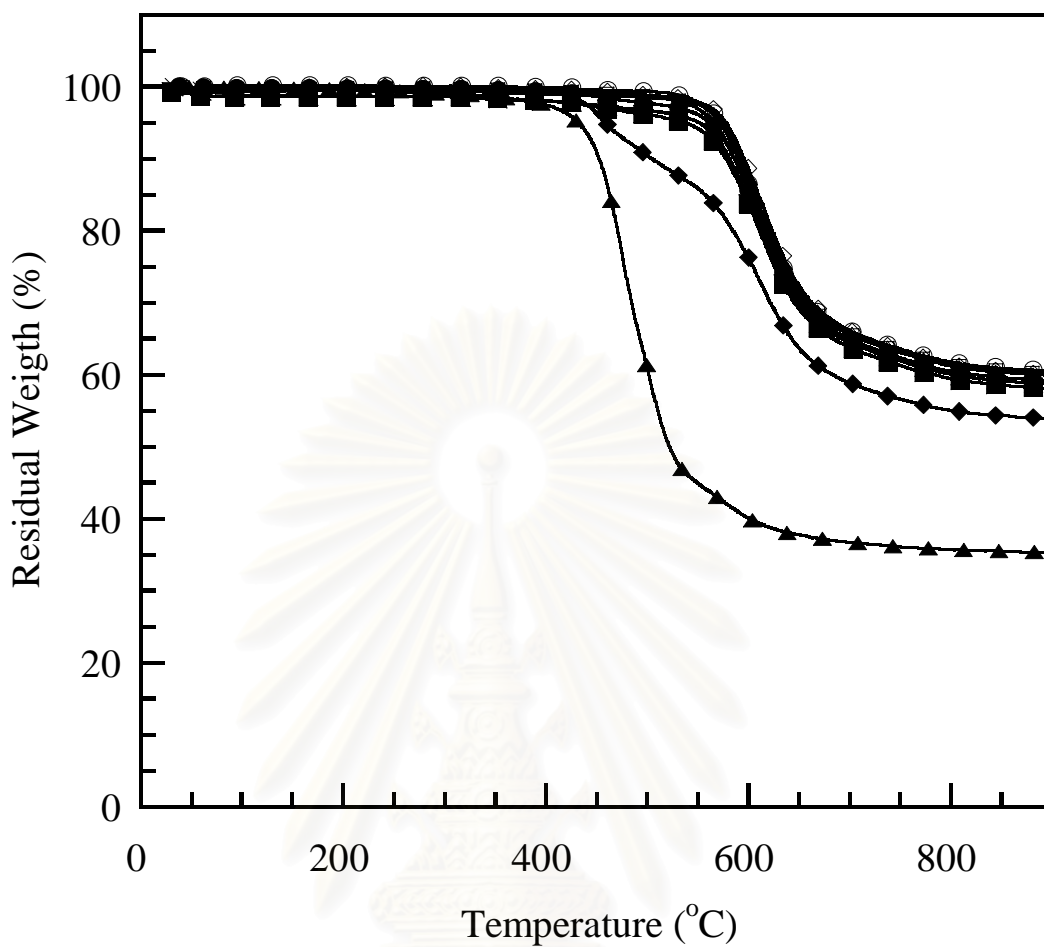


Figure 5.4: TGA thermograms of s-BPDA/ODA polyimide, BSF30, and their blends as a function of BSF30 compositions: (○) s-BPDA/ODA polyimide, (Δ) 0.5 phr, (□) 1 phr, (◇) 2 phr, (×) 3 phr, (●) 4 phr, (■) 5 phr, (◆) 30 phr, and (▲) BSF30.

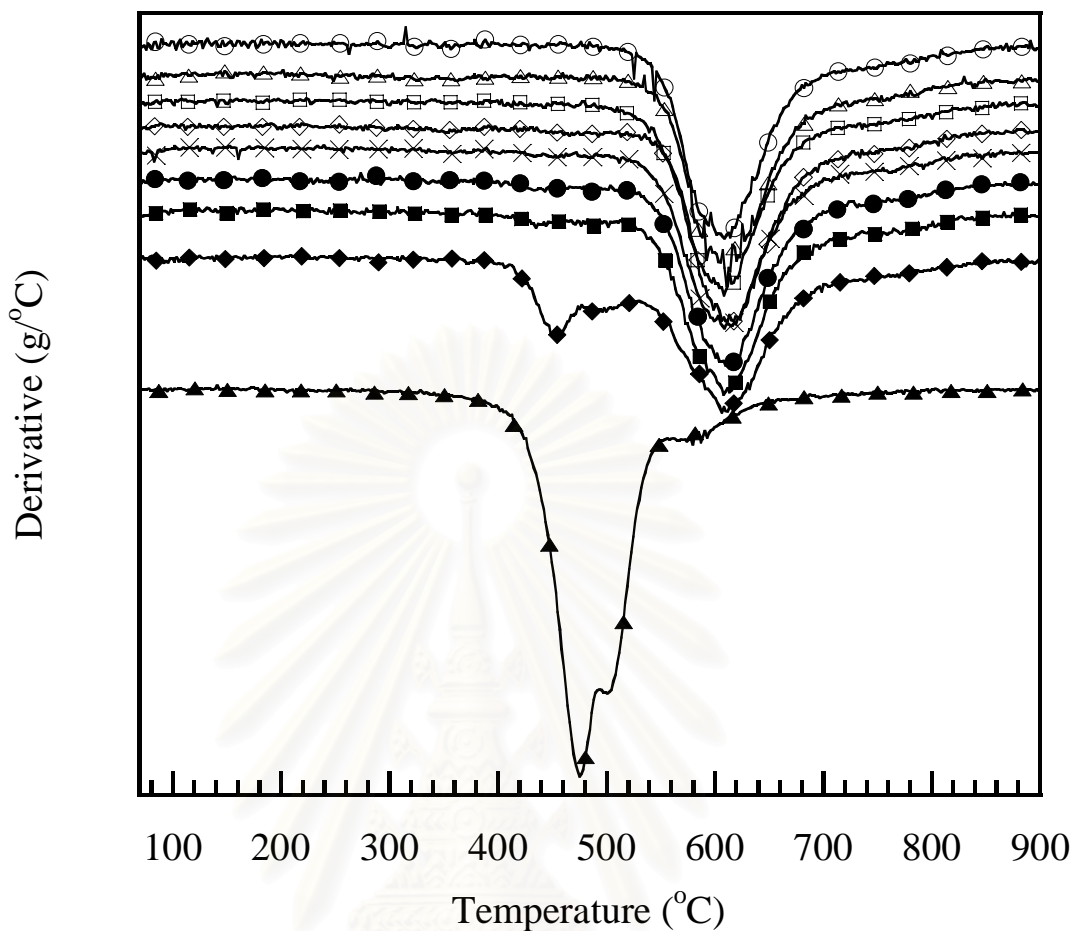


Figure 5.5: DTG thermograms of s-BPDA/ODA polyimide, BSF30, and their blends as a function of BSF30 compositions: (○) s-BPDA/ODA polyimide, (Δ) 0.5 phr, (□) 1 phr, (◇) 2 phr, (×) 3 phr, (●) 4 phr, (■) 5 phr, (◆) 30 phr, and (▲) BSF30.

สถาบันวิทยบริการ
จุฬาลงกรณ์มหาวิทยาลัย

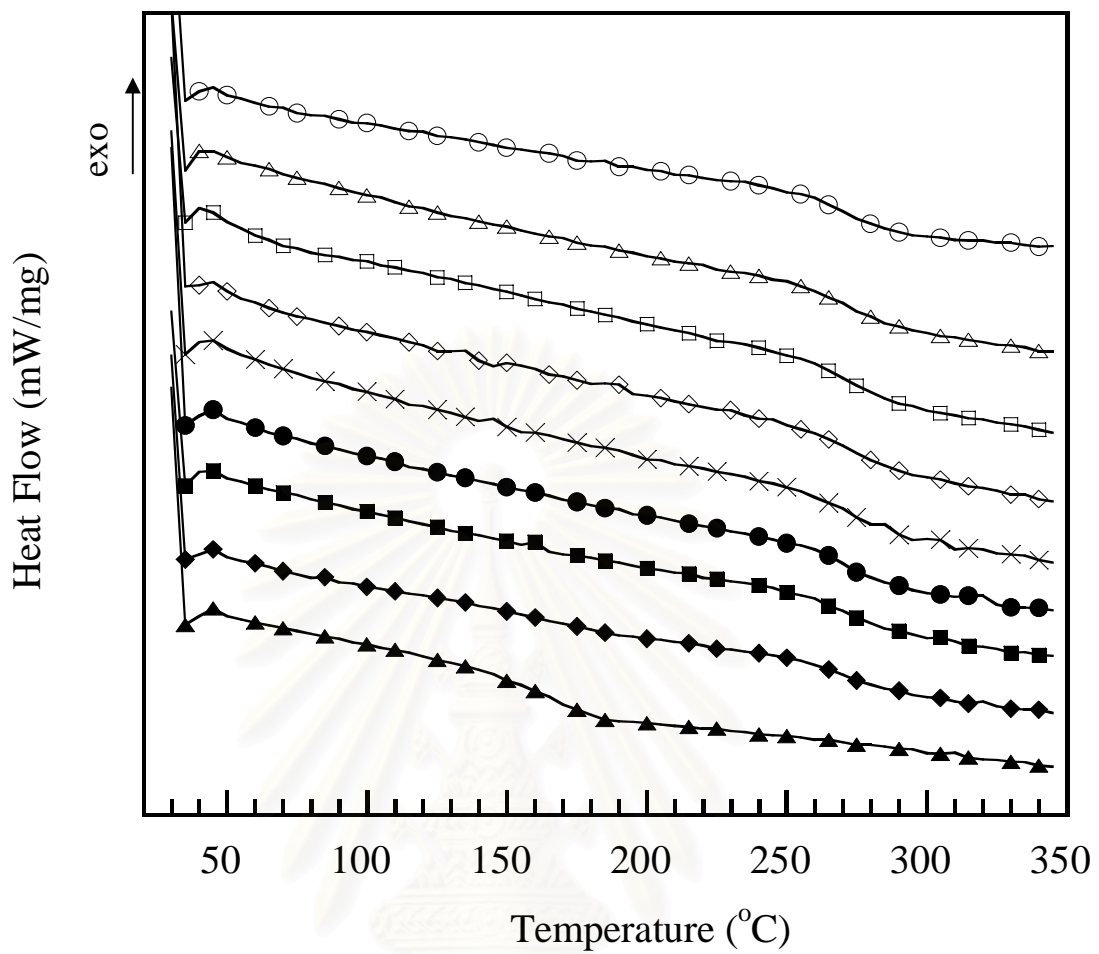


Figure 5.6: DSC thermograms of s-BPDA/ODA polyimide, BSF30, and their blends as a function of BSF30 compositions: (○) s-BPDA/ODA polyimide, (△) 0.5 phr, (□) 1 phr, (◇) 2 phr, (×) 3 phr, (●) 4 phr, (■) 5 phr, (◆) 30 phr, and (▲) BSF30.

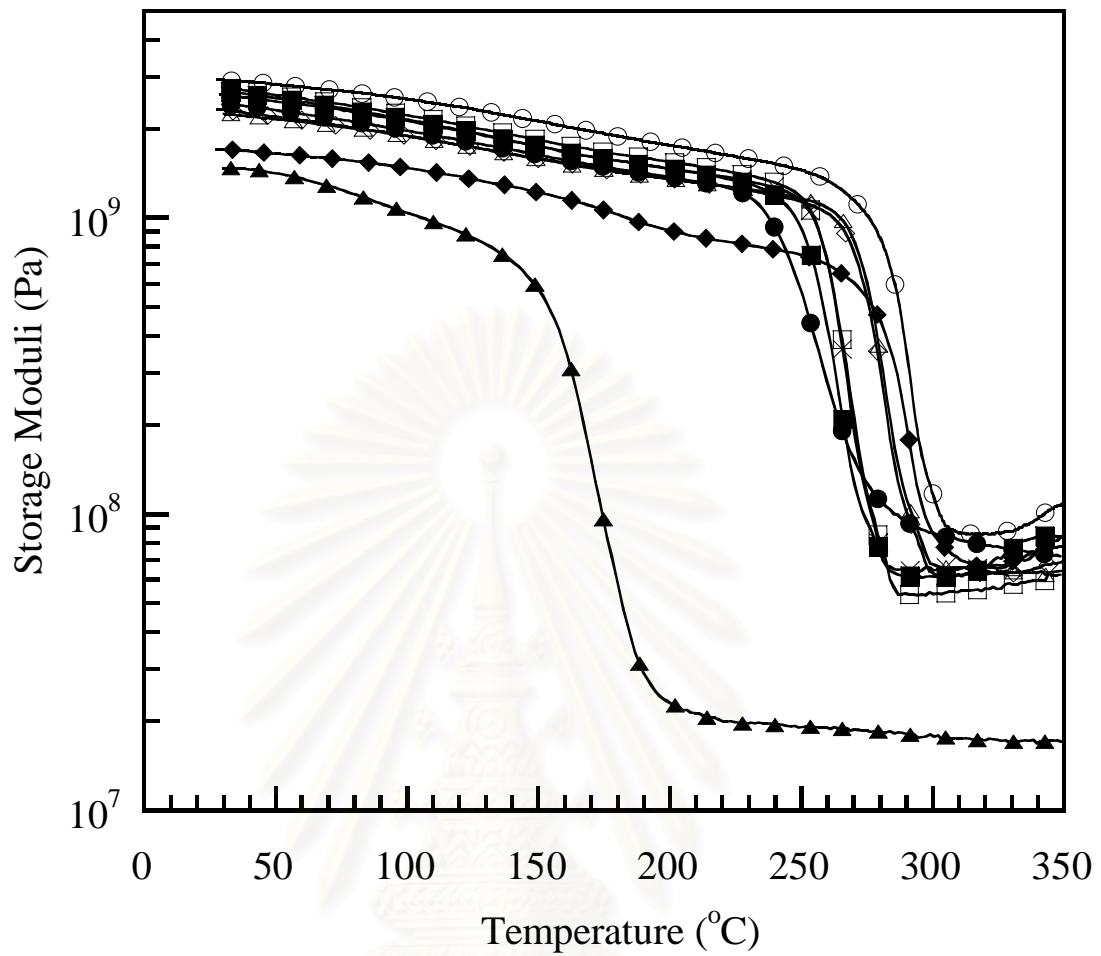


Figure 5.7: Storage moduli of s-BPDA/ODA polyimide, BSF30, and their blends as a function of BSF30 compositions: (○) s-BPDA/ODA polyimide, (△) 0.5 phr, (□) 1 phr, (◇) 2 phr, (×) 3 phr, (●) 4 phr, (■) 5 phr, (◆) 30 phr, and (▲) BSF30.

จุฬาลงกรณ์มหาวิทยาลัย

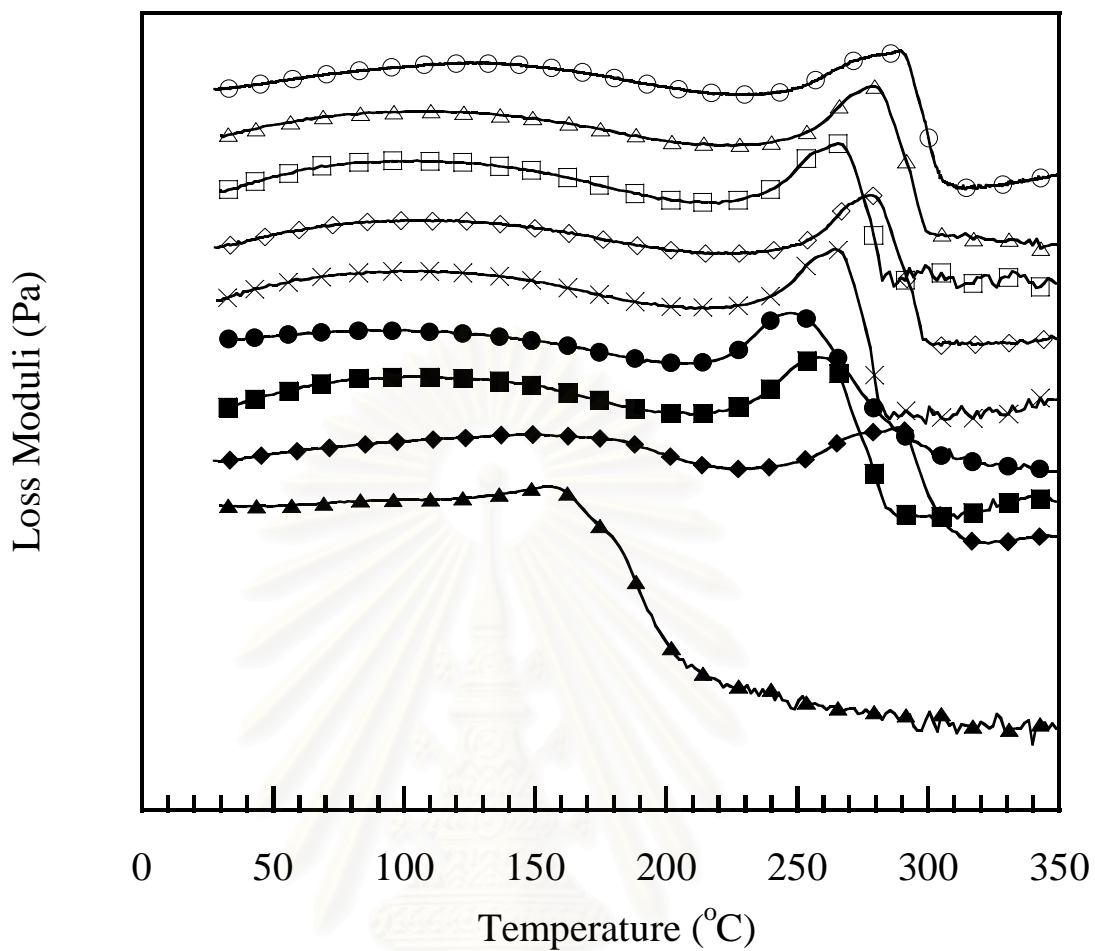


Figure 5.8: Loss moduli of s-BPDA/ODA polyimide, BSF30, and their blends as a function of BSF30 compositions: (○) s-BPDA/ODA polyimide, (△) 0.5 phr, (□) 1 phr, (◇) 2 phr, (×) 3 phr, (●) 4 phr, (■) 5 phr, (◆) 30 phr, and (▲) BSF30.

จุฬาลงกรณ์มหาวิทยาลัย

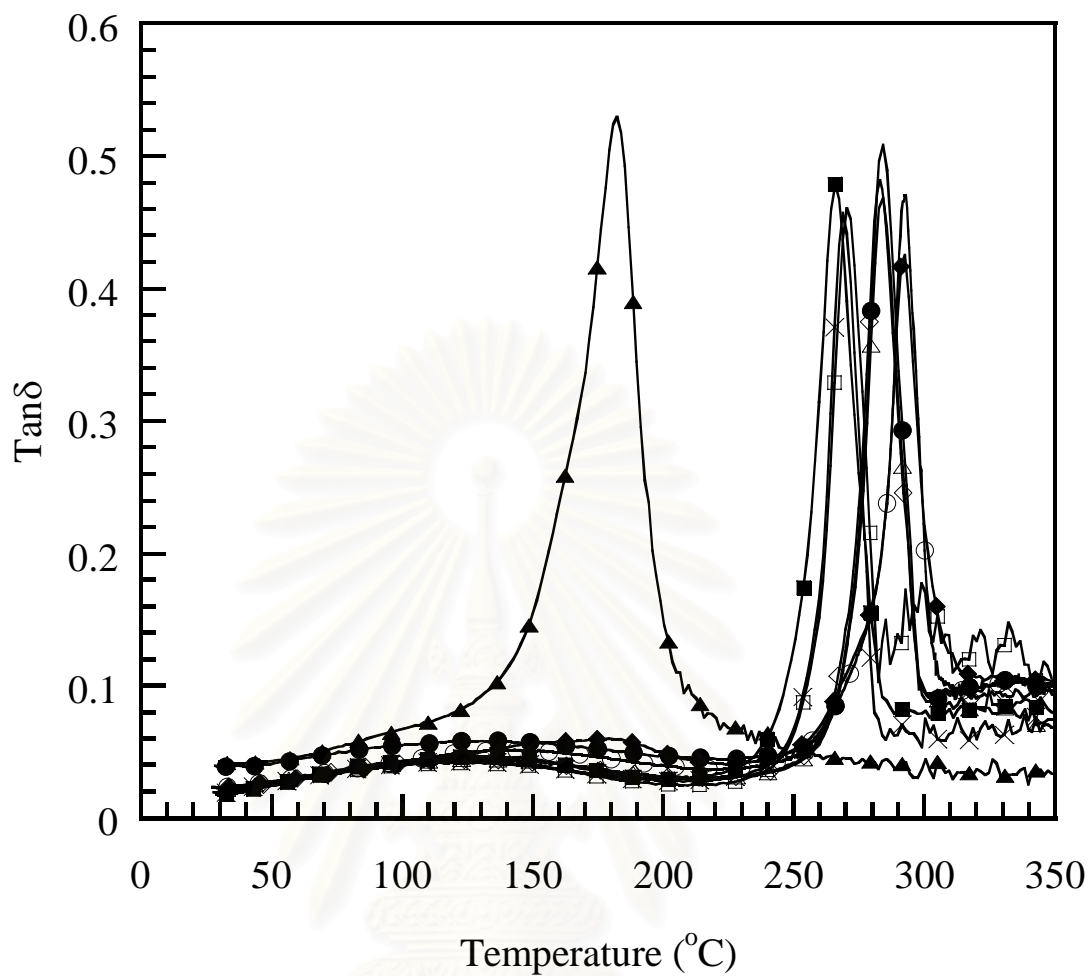


Figure 5.9: Loss tangent of s-BPDA/ODA polyimide, BSF30, and their blends as a function of BSF30 compositions: (○) s-BPDA/ODA polyimide, (Δ) 0.5 phr, (□) 1 phr, (◇) 2 phr, (×) 3 phr, (●) 4 phr, (■) 5 phr, (◆) 30 phr, and (▲) BSF30.

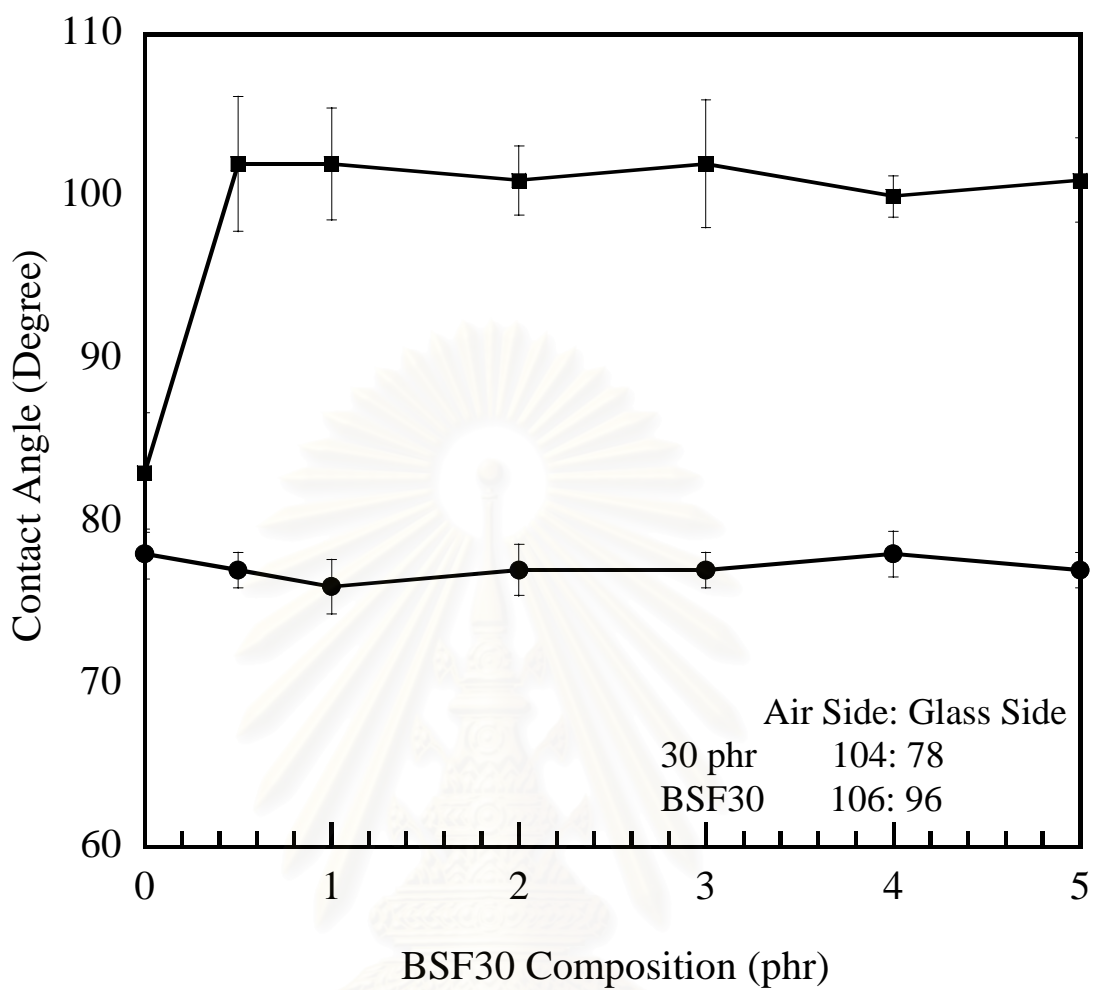


Figure 5.10: Contact angle measurements obtained for water drops on of s-BPDA/ODA polyimide, BSF30, and their blends as a function of BSF30 compositions: (■) Air side, and (●) Glass side.

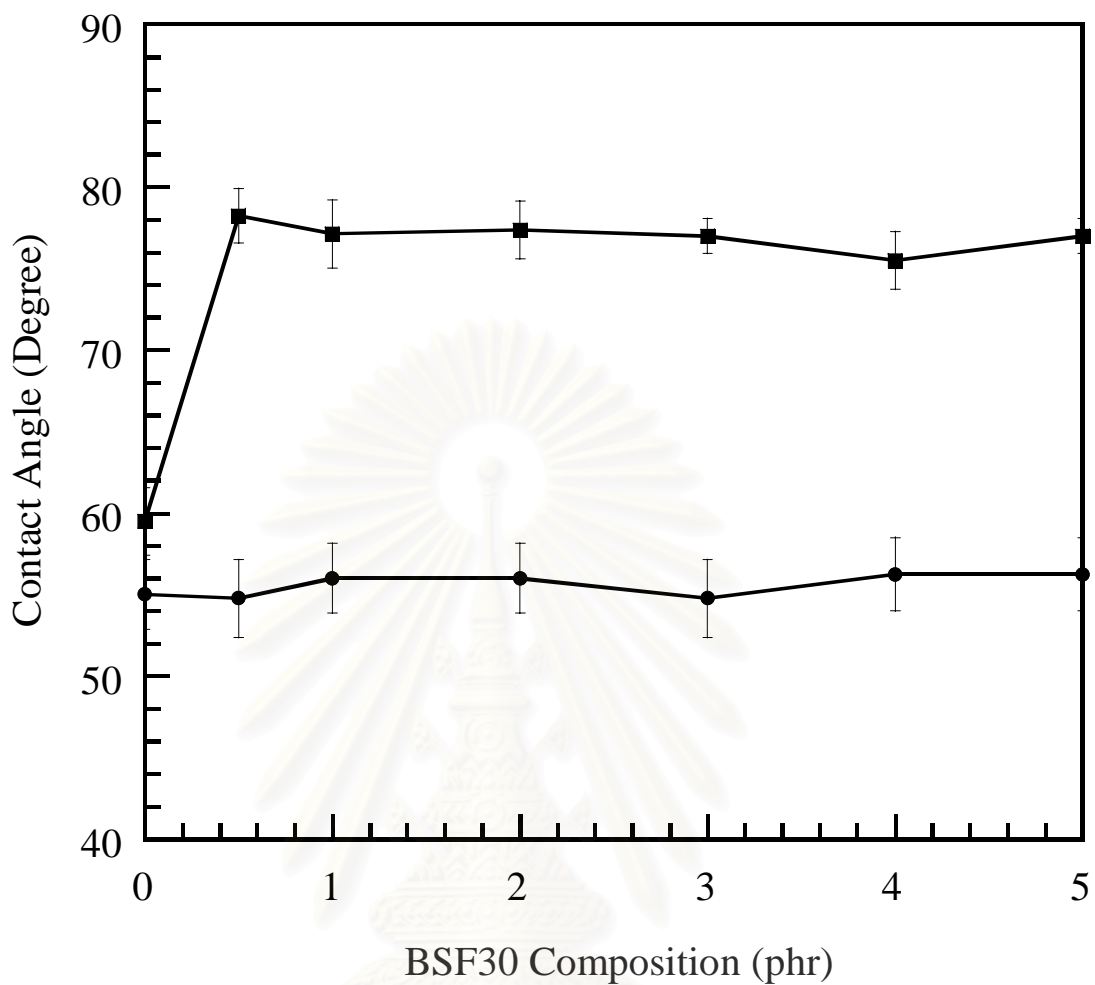


Figure 5.11: Contact angle measurements obtained for ethylene glycol drops on s-BPDA/ODA polyimide, BSF30, and their blends as a function of BSF30 compositions: (■) Air side, and (●) Glass side.

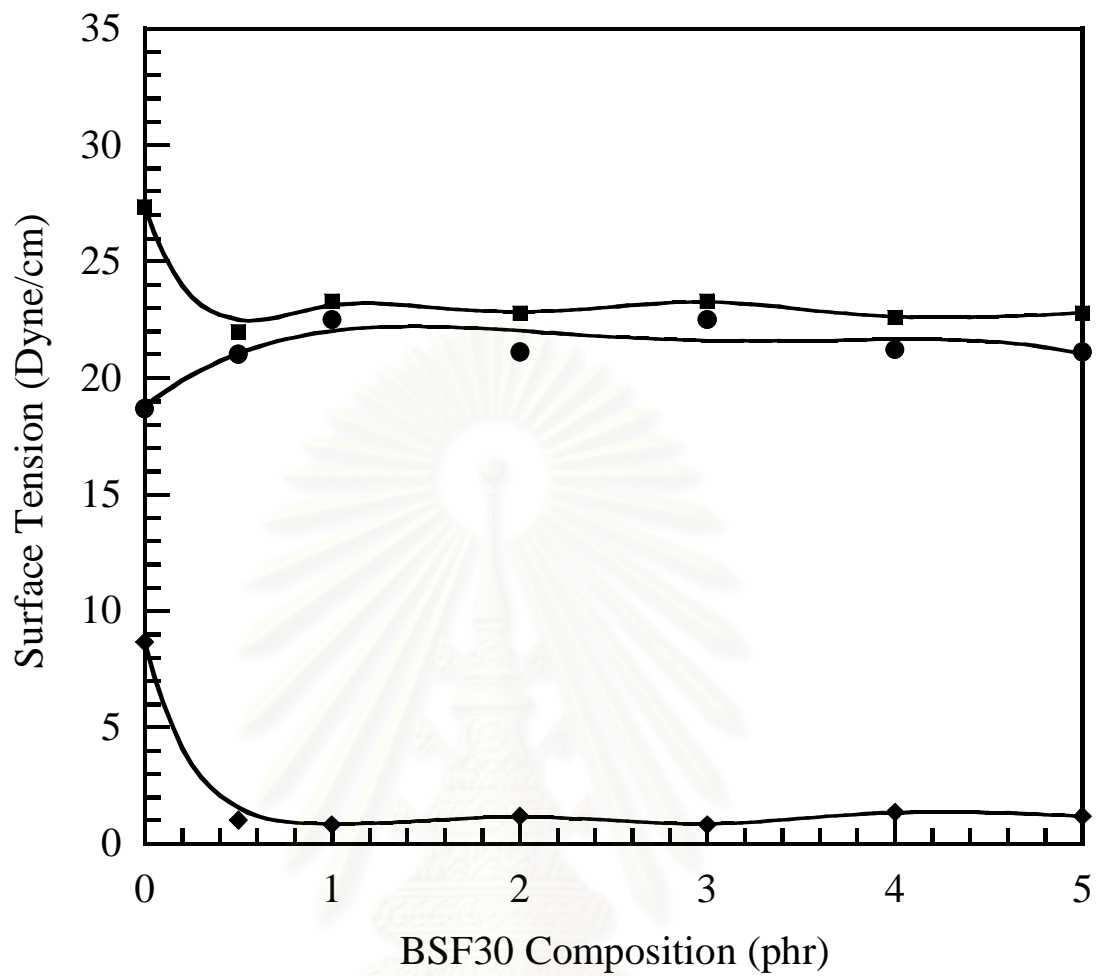


Figure 5.12: Surface tension of s-BPDA/ODA polyimide, BSF30, and their blends as a function of BSF30 compositions: (■) Surface Tension, (●) Dispersion component of surface tension, and (◆) Polar component of surface tension.

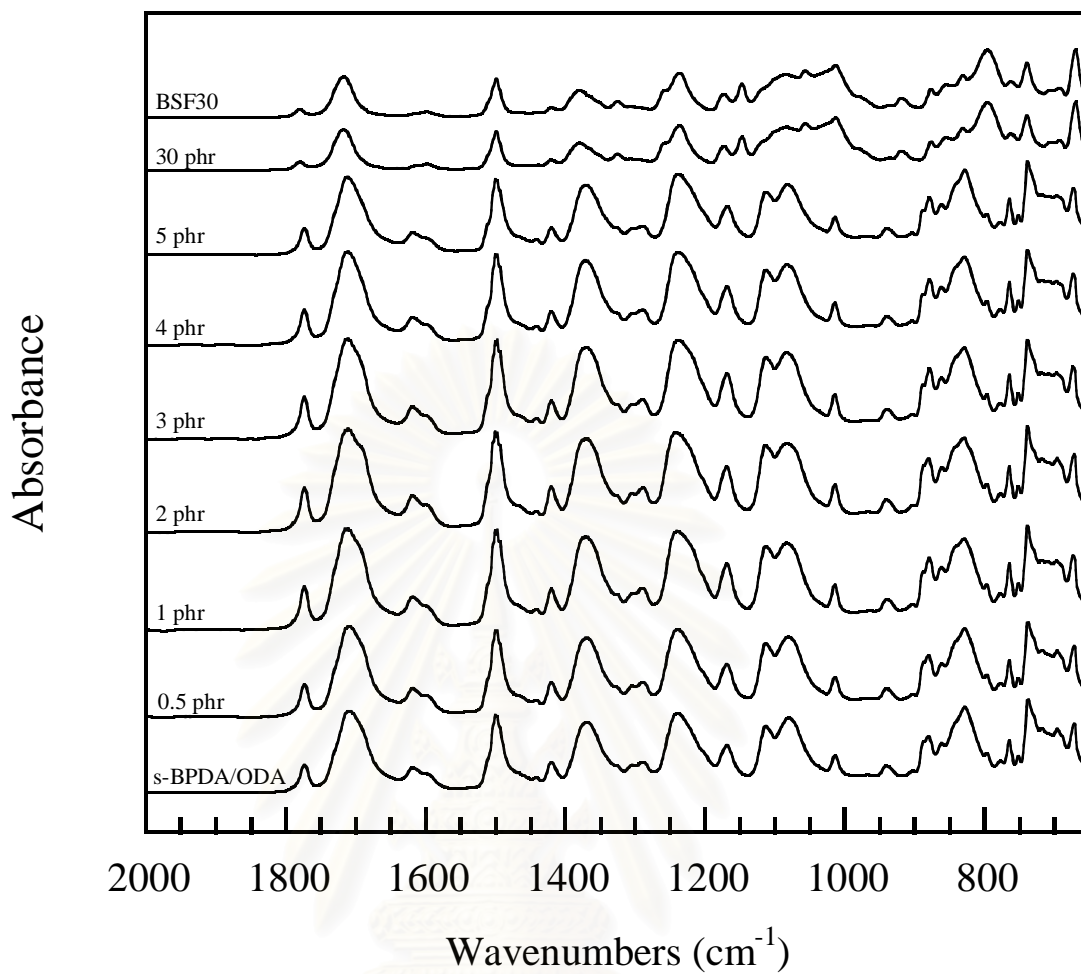


Figure 5.13: ATR-FTIR spectra s-BPDA/ODA polyimide, BSF30, and their blends as a function of BSF30 composition as a function of the BSF30 compositions on glass substrate (Air side).

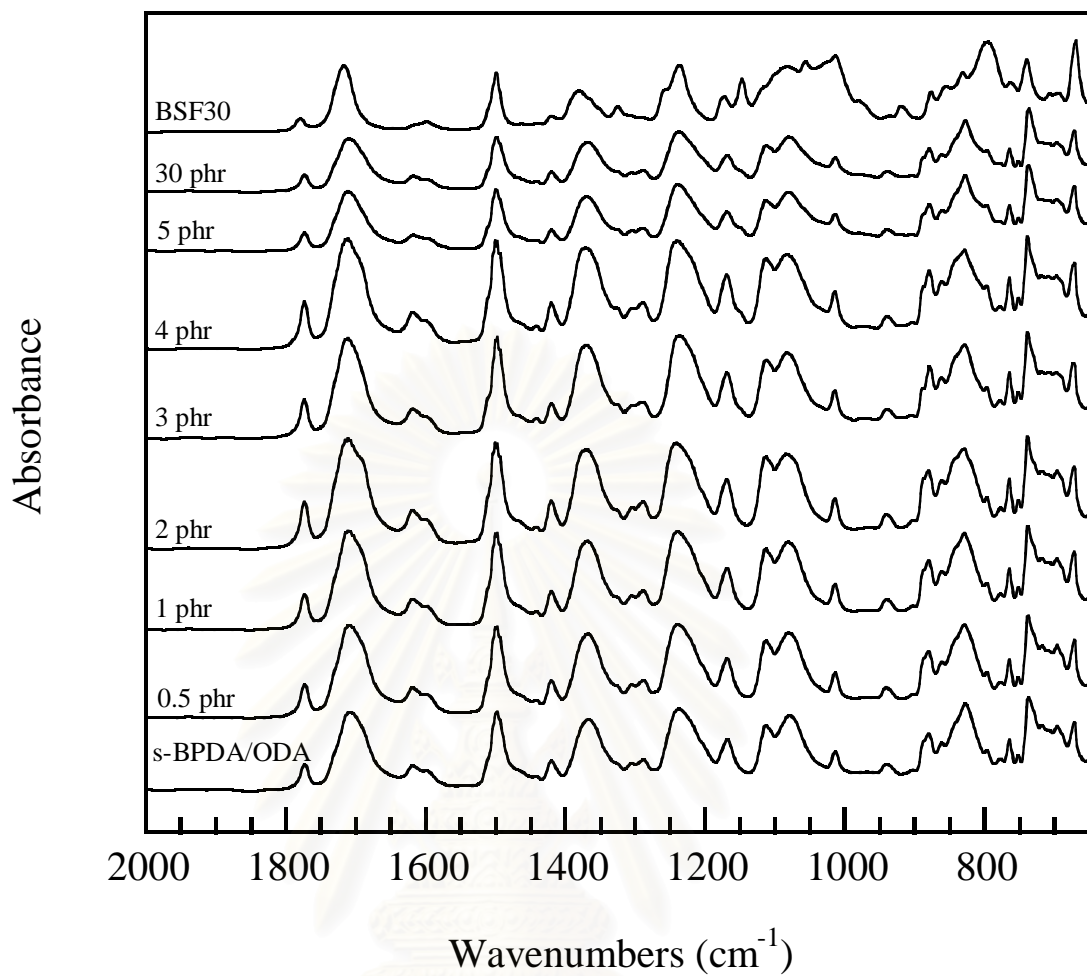


Figure 5.14: ATR-FTIR spectra s-BPDA/ODA polyimide, BSF30, and their blends as a function of BSF30 compositions on glass substrate (Glass side).

สถาบันทศบริการ
จุฬาลงกรณ์มหาวิทยาลัย

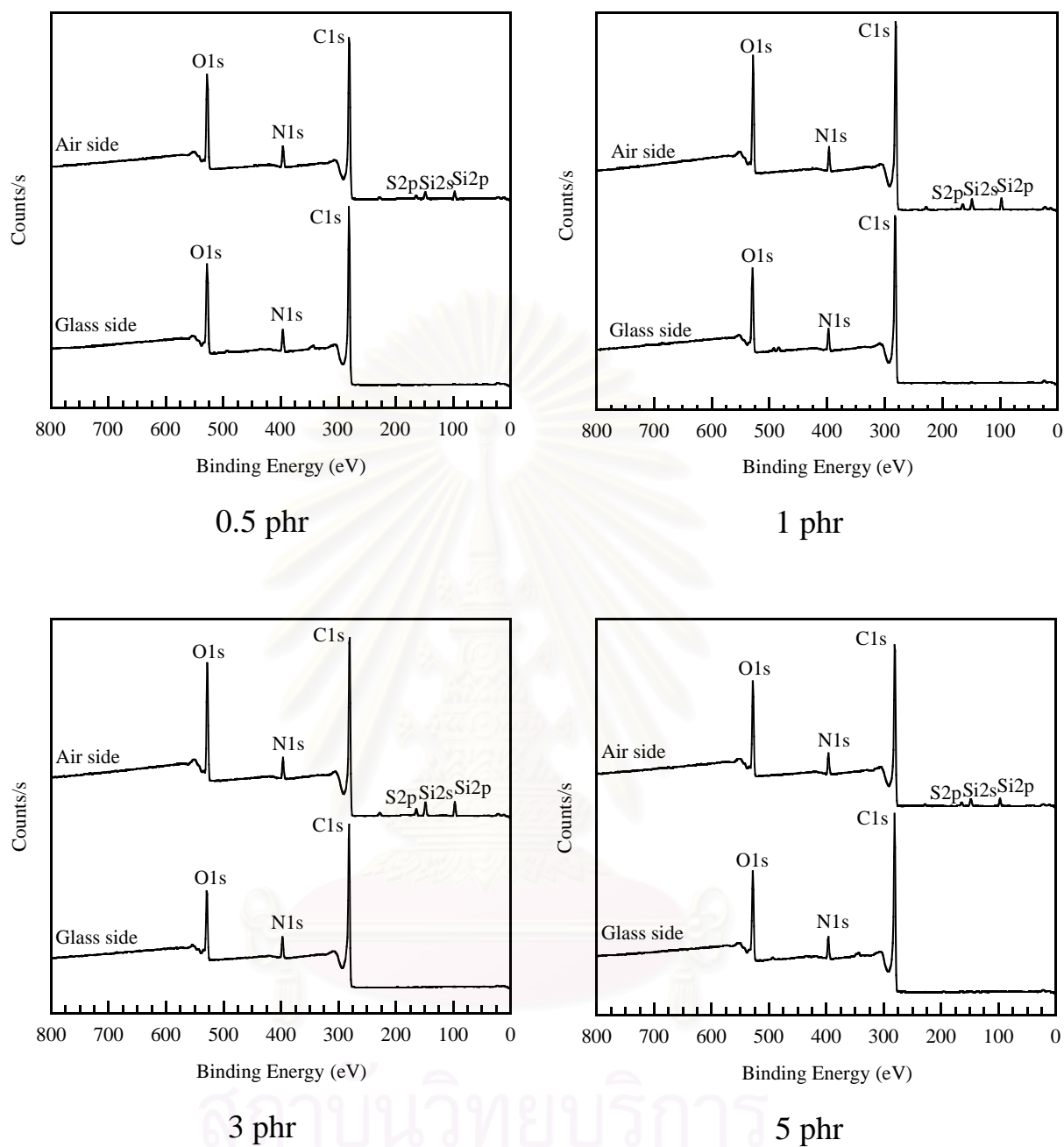


Figure 5.15: XPS survey scans of s-BPDA/ODA polyimide, BSF30, and their blends as a function of BSF30 compositions on glass substrate.

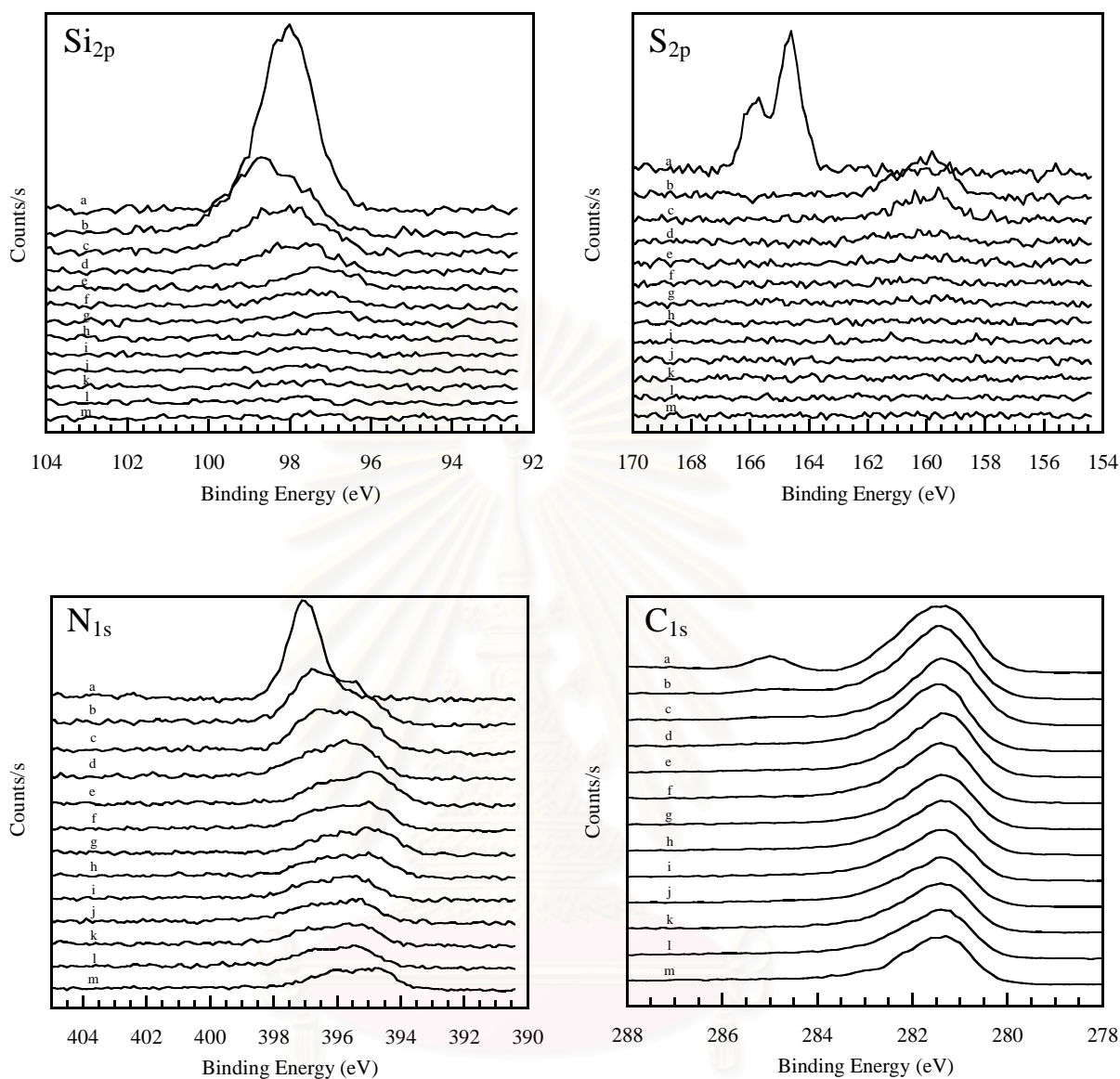


Figure 5.16: XPS depth profiling showing Si_{2p} , S_{2p} , N_{1s} , C_{1s} , and O_{1s} peaks of 0.5 phr of BSF30: (a) 0 sec, (b) 15 sec, (c) 30 sec, (d) 45 sec, (e) 60 sec, (f) 75 sec, (g) 90 sec, (h) 105 sec, (i) 120 sec, (j) 135 sec, (k) 150 sec, (l) 165 sec, (m) 180 sec.

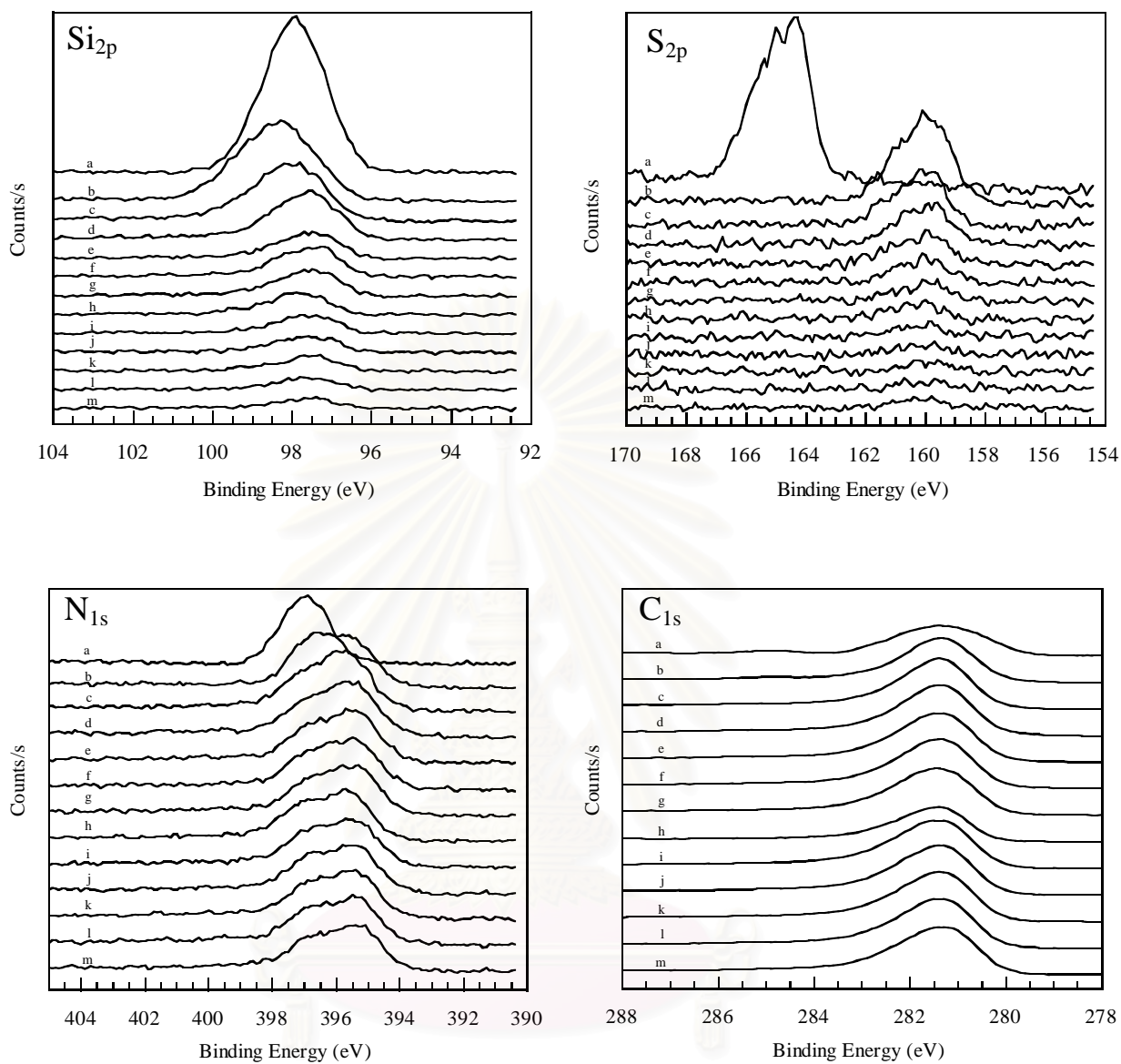


Figure 5.17: XPS depth profiling showing Si_{2p} peaks of 5 phr BSF30: (a) 0 sec, (b) 15 sec, (c) 30 sec, (d) 45 sec, (e) 60 sec, (f) 75 sec, (g) 90 sec, (h) 105 sec, (i) 120 sec, (j) 135 sec, (k) 150 sec, (l) 165 sec, (m) 180 sec.

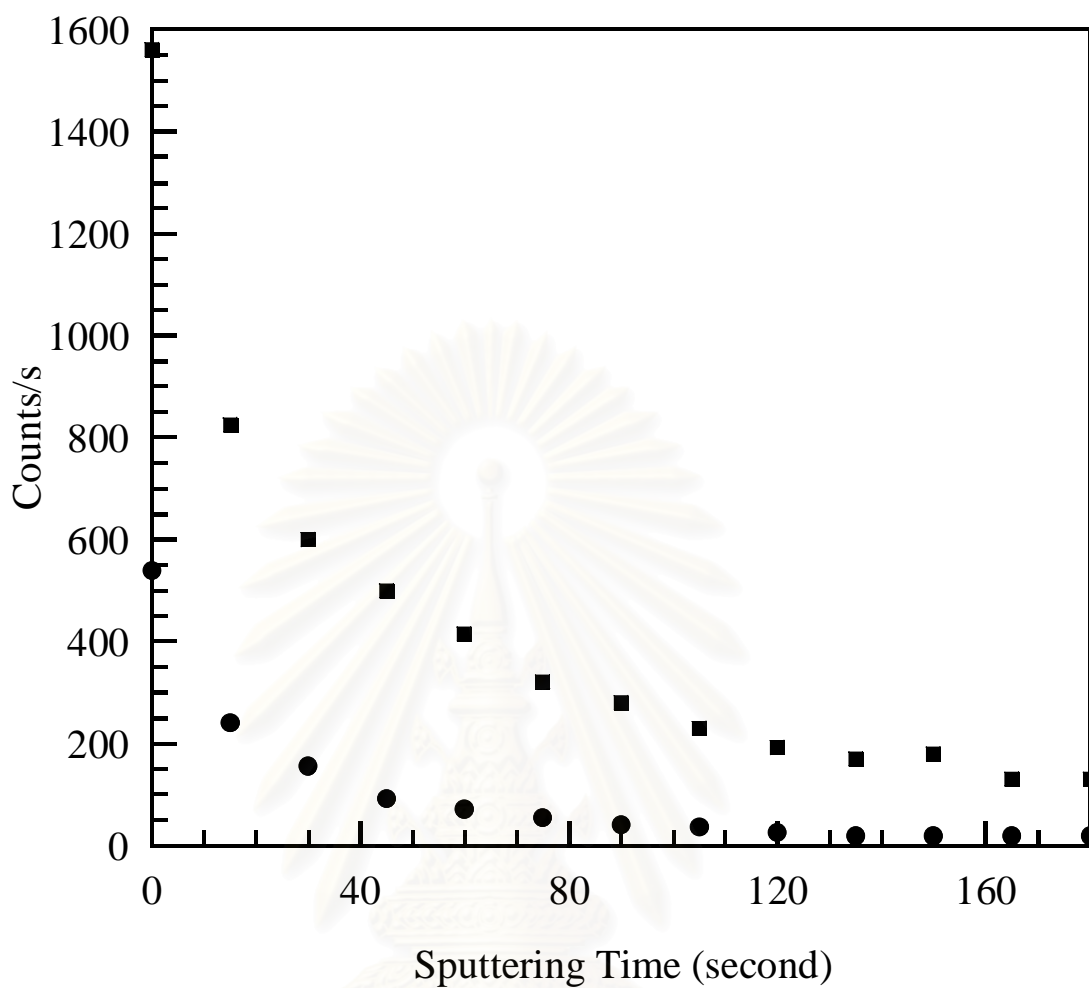


Figure 5.18: Changes of XPS peaks of Si_{2p} of 0.5 phr and 5 phr of BSF30 with time of sputtering: (■) 0.5 phr, (●) 5 phr.

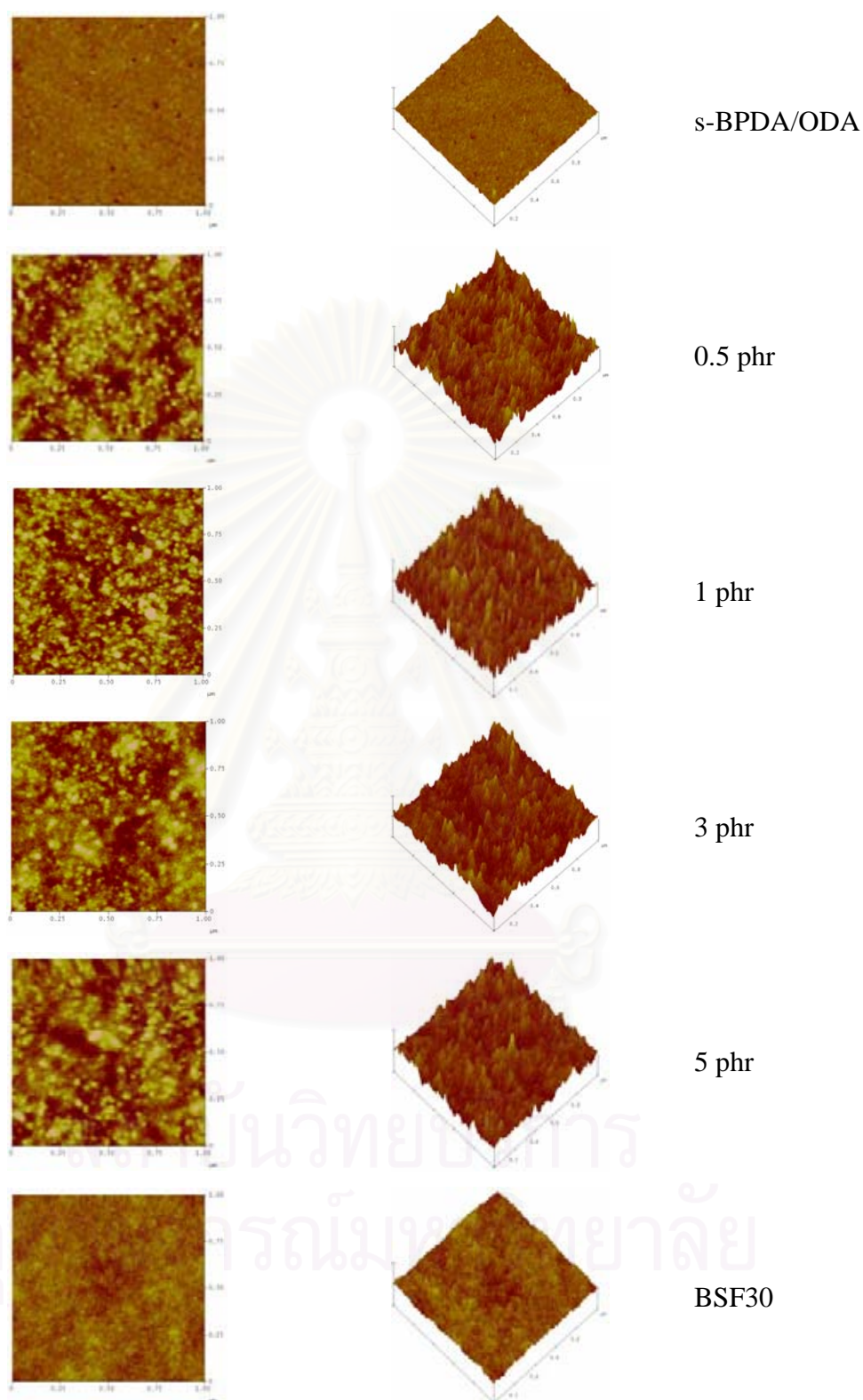
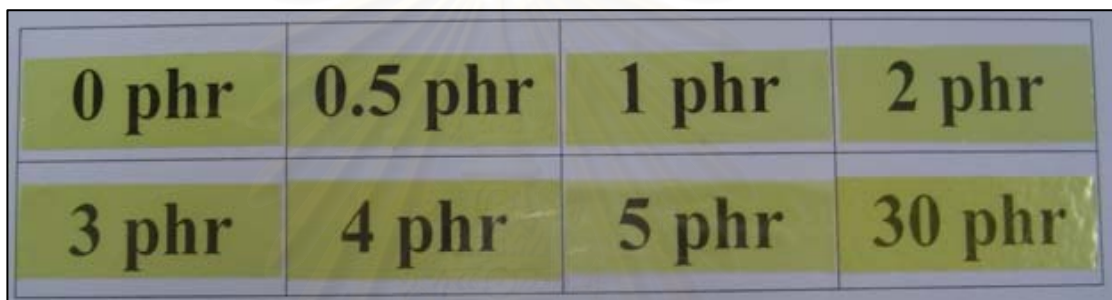


Figure 5.19: AFM high images of s-BPDA/ODA polyimide, BSF30, and their blends as a function of BSF30 compositions (z-axis = 10 nm).



0 phr	0.5 phr	1 phr	2 phr
3 phr	4 phr	5 phr	30 phr

Figure 5.20: s-BPDA/ODA polyimide, BSF30, and their blends as a function of BSF30 compositions.

สถาบันวิทยบริการ
จุฬาลงกรณ์มหาวิทยาลัย

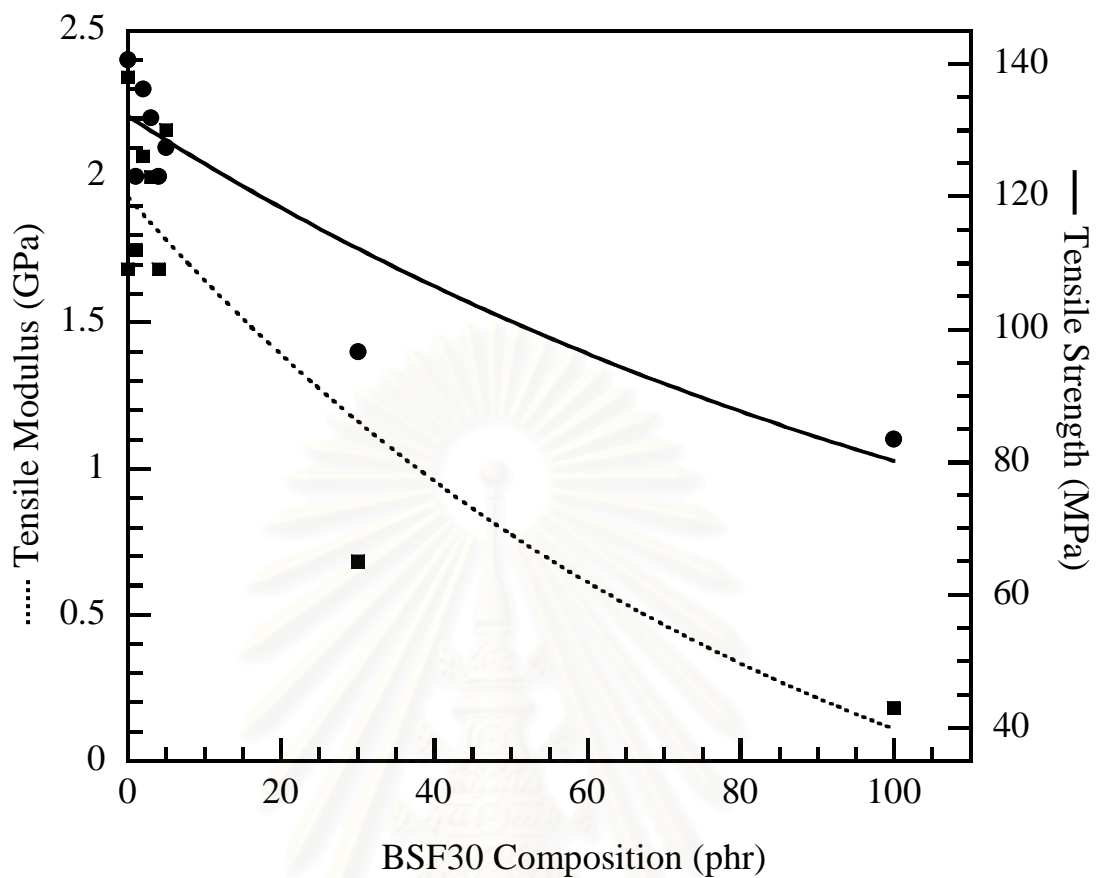


Figure 5.21: Mechanical properties of s-BPDA/ODA polyimide, BSF30, and their blends as a function of BSF30 compositions: (··■··) Tensile Modulus and (—●—) Tensile Strength.

สถาบันวิทยบริการ
จุฬาลงกรณ์มหาวิทยาลัย

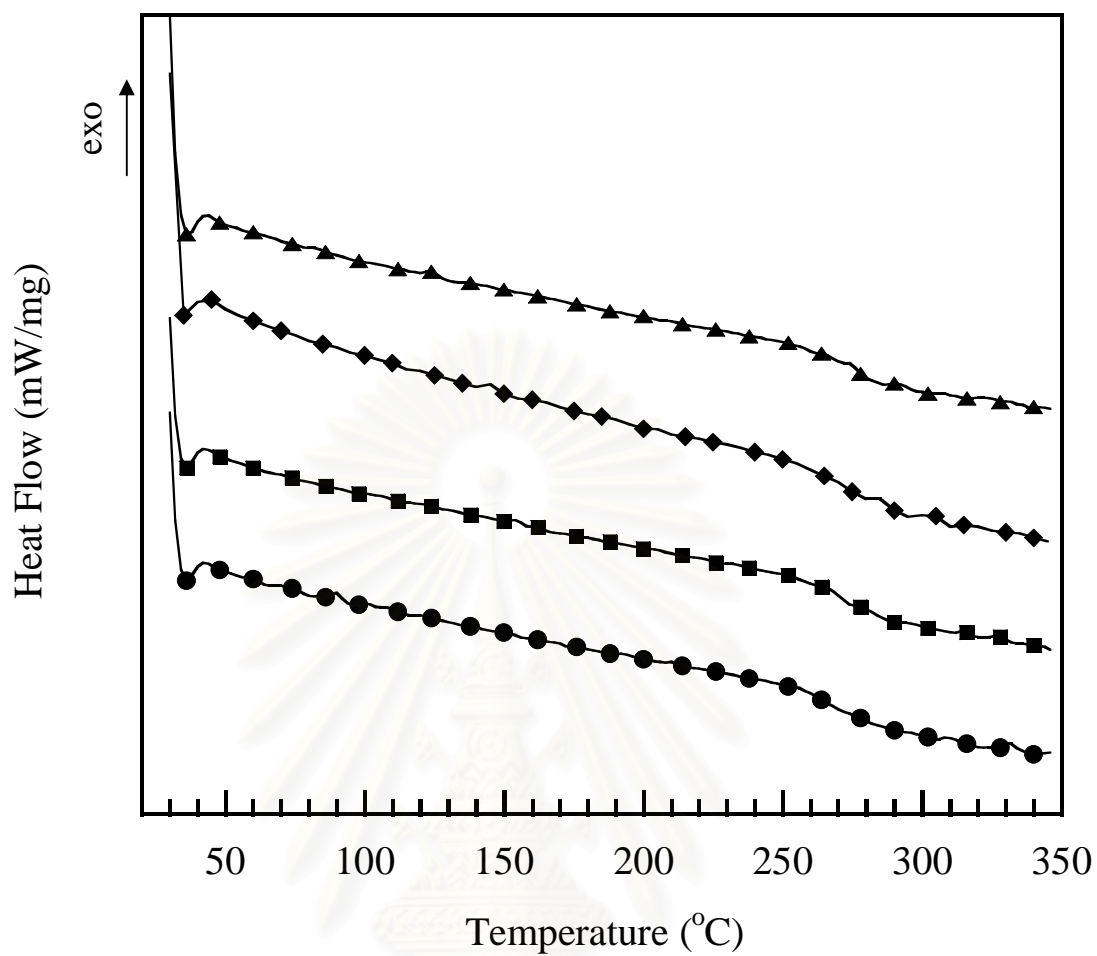


Figure 5.22: DSC Thermograms of 3 phr of BSF30 at various cosolvent compositions: (●) 0%, (■) 50%, (◆) 100%, and (▲) 150%.

สถาบันวิทยบริการ
จุฬาลงกรณ์มหาวิทยาลัย

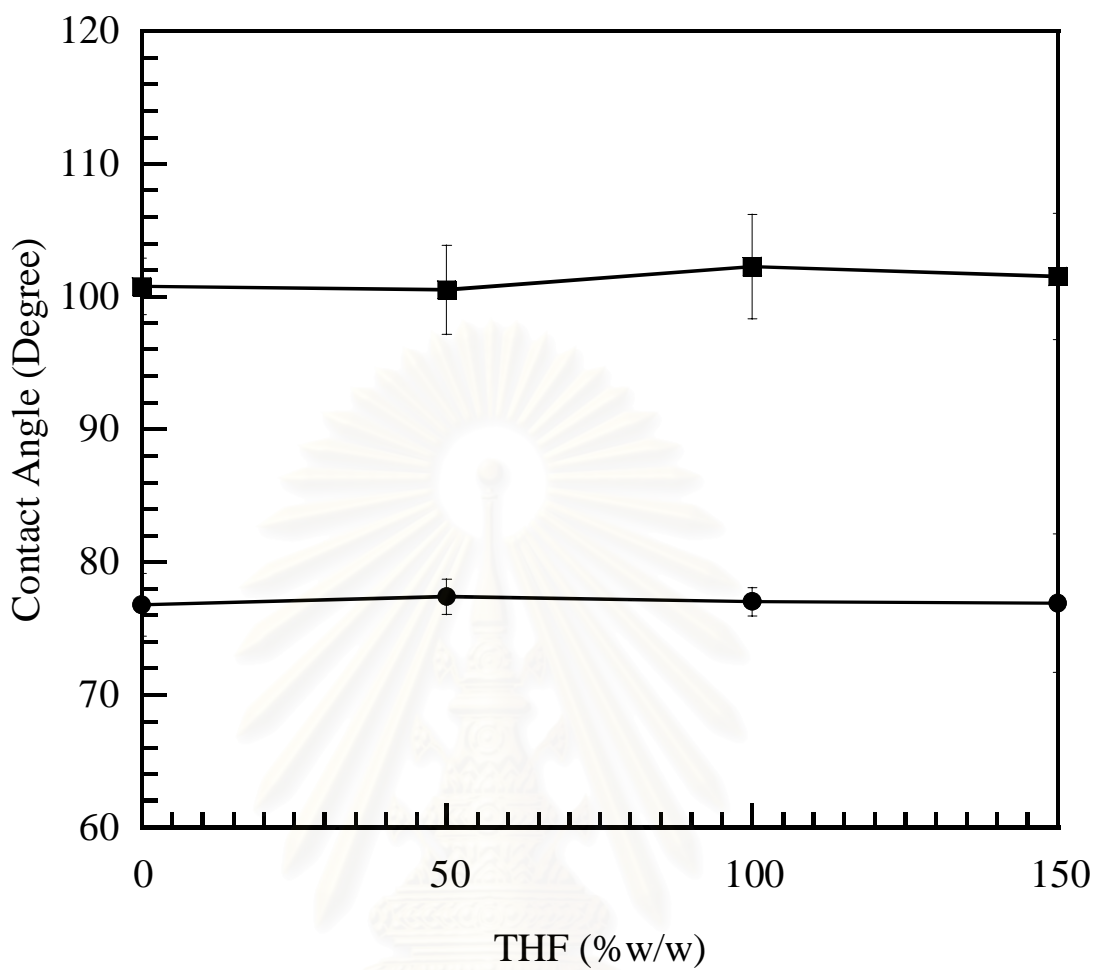


Figure 5.23: Contact angle measurements of 3 phr of BSF30 at various cosolvent compositions.

สถาบันวิทยบริการ
จุฬาลงกรณ์มหาวิทยาลัย

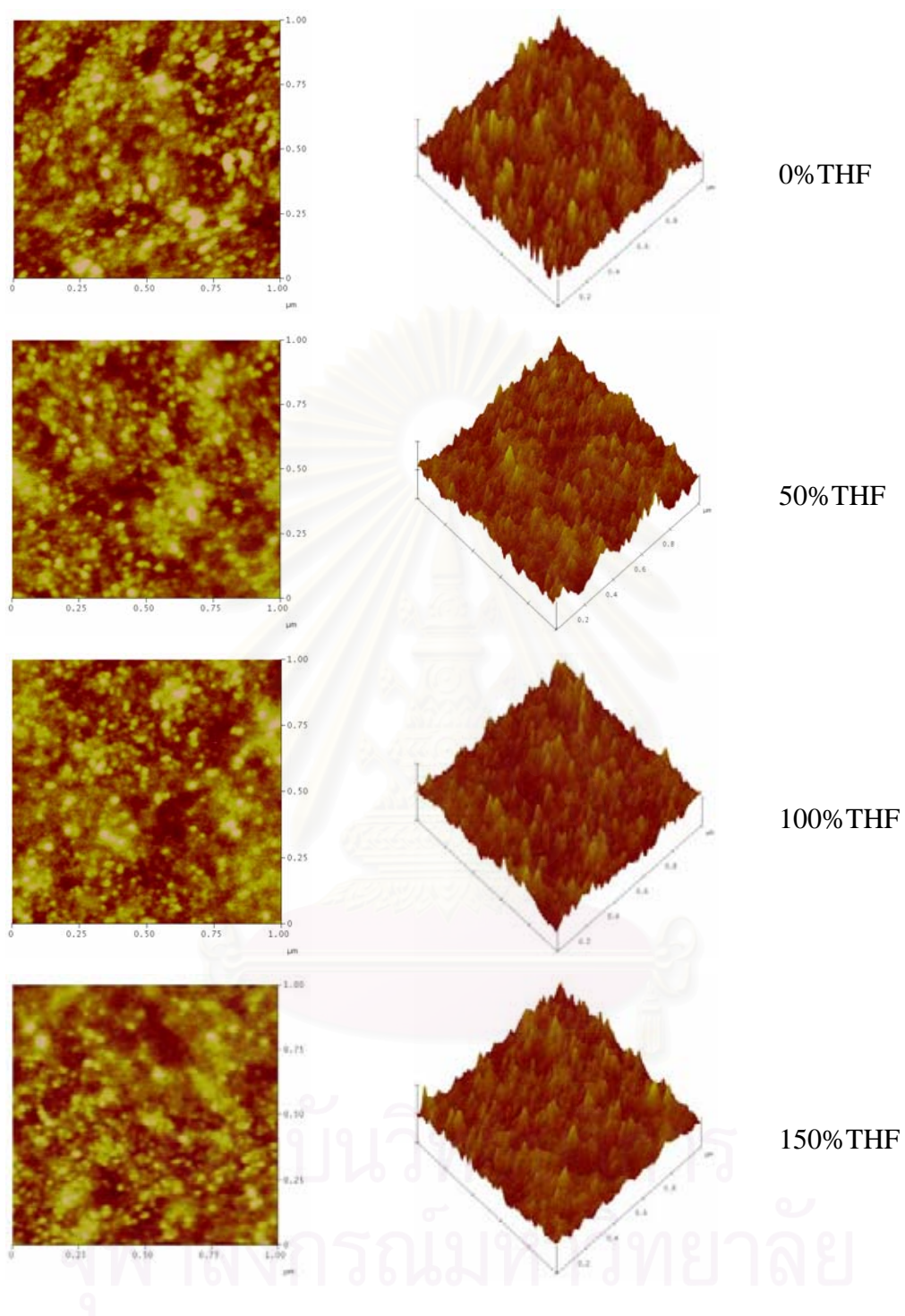


Figure 5.24: AFM high images of 3 phr of BSF30 at various cosolvent compositions (z-axis = 10 nm).

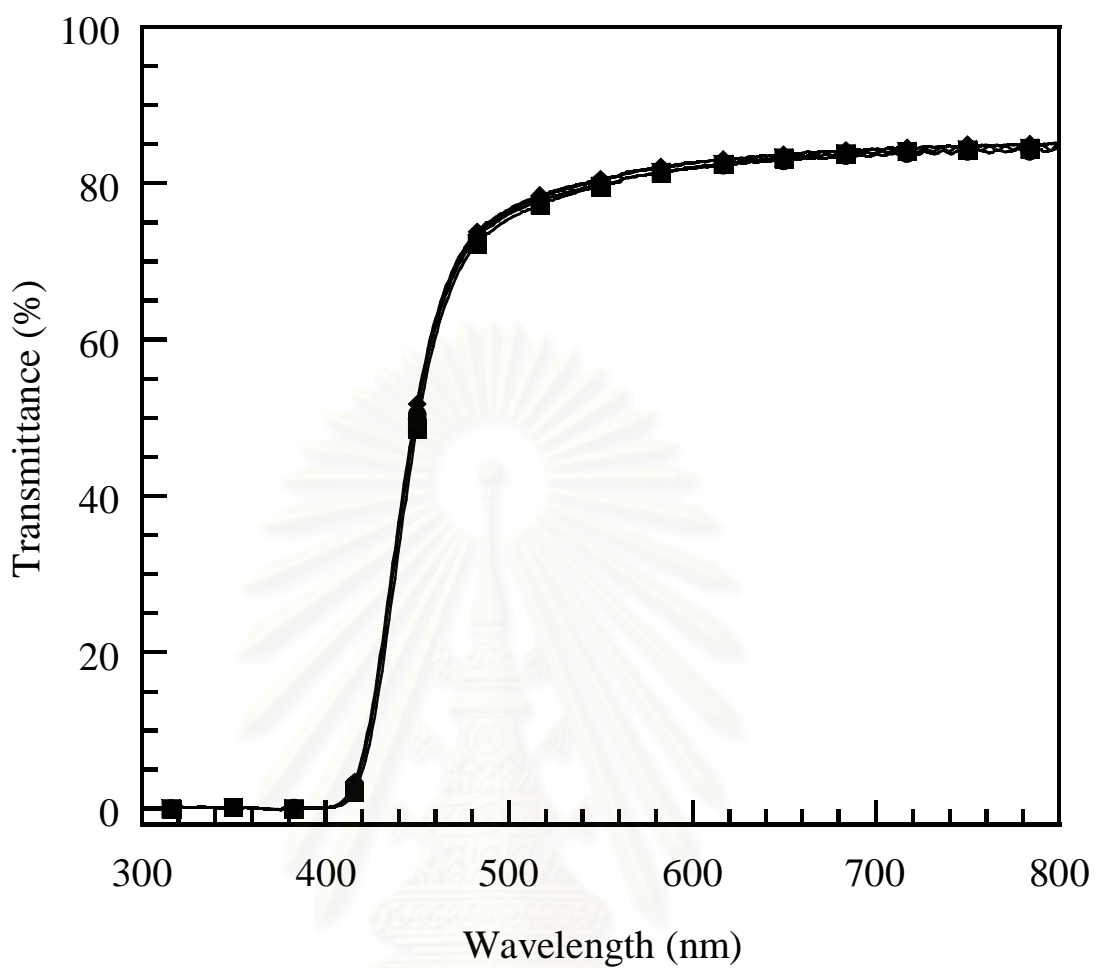


Figure 5.25: UV-visible spectra of 3 phr of BSF30 blends at various cosolvent compositions: (●) 0%, (■) 50%, (◆) 100%, and (▲) 150%.

สถาบันวิทยบริการ
จุฬาลงกรณ์มหาวิทยาลัย

CHAPTER VI

CONCLUSIONS

Surface modification of s-BPDA/ODA polyimide through mixing of BSF30 was investigated by using various measurement techniques, i.e. from contact angle, ATR-FTIR, AFM, and XPS. Because of the lower surface tension of the BSF30 fraction compared to the s-BPDA/ODA fraction, surface segregation of the BSF30 was found in all blend compositions. These results are attributed to the low surface tension of the siloxane moieties in the BSF30 (21-22 dyne/cm), which tended to migrate to the air-polymer interface and form a siloxane-enriched surface. This siloxane-enriched surface could be formed even when the BSF30 content was relatively low (0.5 phr). An addition of small amount of the BSF30 (0.5-5 phr) showed no significant effect on the bulk properties and the transparency of the blend films. XPS depth profiling showed that the Si concentration was very high at the top surface. Thereafter, the Si concentration gradually decreased with depth of the film in an exponential decay manner. An increase in the BSF30 composition was found to result in an increase in the thickness of the silicone-riched surface layer. At the low BSF30 composition (0.5-5 phr), there was no significant effect on the thermal and mechanical properties such as degradation temperature, char yield, glass transition temperature, and mechanical properties. Finally, the amount of cosolvent showed no effect on the surface properties of blend films.

สภานิติบัญญัติ
จุฬาลงกรณ์มหาวิทยาลัย

REFERENCES

- Andre, S.; Guida-Pietrasanta, F.; Rousseau, A.; and Boutevin, B. Novel synthesis of polyimide-polyhybridsiloxane block copolymers via polyhydrosilylation: Characterization and physical properties. J. Polym. Sci., Part A: Polym. Chem. 39 (2001): 2414-2425.
- Arnold, C. A., Summers, J. D., Chen, Y. P., Yoon, T. H., McGrath, B. E., Chen, D., and McGrath, J.E., Polyimides: Materials, Chemistry and Characterization. Amsterdam: Elsevier Science Publishers B.V., 1989.
- Banks, B. A. and Denko, R. Proc. SAMPE 2002, MAY 12-16, 2002, Long Beach, California.
- Bowens, A. D. Synthesis and Characterization of Poly(siloxane imide) Block Copolymers and End-Functional Polyimides for Interphase Applications. Doctoral dissertation, Chemistry, Virginia Polytechnic Institute and State University, (1999).
- Cassie, A. B. D. Contact Angle. Discussion Faraday Soc 3 (1948): 11-16.
- Child, C. M.; Fieberg, J. E.; and Campion, A. Surface Chemistry of Polyimide Formation on Cu(111). Surface Science 372 (1997): 254-260
- Chen, J. and Gardella, J. A. Solvent Effects on the Surface Composition of Poly(dimethylsiloxane) – co – Polystyrene / Polystyrene Blends. Macromolecules 31 (1998): 9328-9336.
- Chen, X. and Gardella, J. A. Surface Modification of Polymers by Blending Siloxane Block Copolymers. Macromolecules 27 (1994): 3363-3369.
- Chen, X.; Gardella, J. A.; and Kumler, P. L. Surface Morphology Studies of Multiblock and Starblock Copolymers of Poly(α -methylstyrene) and Poly(dimethylsiloxane). Macromolecules 26 (1993): 3778-3783.
- Cho, S. H.; Kim, S. H.; Lee, J. G.; and Lee, N. E. Micro-scale Metallization of High Aspect-ratio Cu and Au Lines on Flexible Polyimide Substrate by Electroplating Using SU-8 Photoresist Mask. Microelectron. Eng. 77 (2005): 116-124.
- Dunson, D. L. Synthesis and Characterization of Thermosetting Polyimide Oligomers for Microelectronics Packaging. Doctoral dissertation, Chemistry, Virginia Polytechnic Institute and State University, (2000).

- Furukawa, N.; Yamada, Y.; Furukawa, M.; Yuasa, M.; and Kimura, Y. Surface and Morphological Characterization of Polysiloxane-Block-Polyimide. J. Polym. Sci., Part A: Polym. Chem. 35 (1997): 2239-2251.
- Gardner, S. H. An Investigation of the Structure-Property Relationships for High Performance Thermoplastic Matrix, Carbon Fiber Composites with a Tailored Polyimide Interphase. Doctoral dissertation, Chemical Engineering, Virginia Polytechnic Institute and State University, (1998).
- Ghosh, M. K., and Mittal, K. L., eds. Polyimides Fundamentals and Applications. New York: Marcel Dekker, 1996.
- Grossman, E. and Gouzman, I. Space Environment Effects on Polymers in Low Earth Orbit. Nucl. Instrum. and Meth. B 208 (2003): 48-57.
- Hatashi, M.; Ribbe, A.; Hashimoto, T.; Weber, M.; and Heckmann, W. The Influence of Wettability on the Morphology of Blends of Polysulfones and Polyamides. Polymer 39 (1998): 299-308.
- Hergenrother, P. M.; Watson, K.A.; Smith, J. G.; Connell, J. W.; and Yokota, R. Polyimides from 2,3,3',4'-Biphenyltetracarboxylic Dianhydride and Aromatic Diamines. Polymer 43 (2002): 5077-5093.
- Hsiao, S. H. and Chen, Y. J. Structure-Property Study of Polyimides Derived from PMDA and BPDA Dianhydrides with Structurally Different Diamines. European Polymer Journal 38 (2002): 815-828.
- Inoue, H.; Matsumoto, A.; Matsukawa, K.; Ueda, A.; and Nagai, S. J. Appl. Polym. Sci. 41 (1990); 1815. Cite in Spanos, C. G.; Ebbens, S. J.; Badyal, J. P. S.; Goodwin, A. J.; and Merlin, P. J. Surface Segregation and Plasma Oxidation of Polyethylene-Poly(dimethylsiloxane) Copolymer Doped Polyethylene Films. Macromolecules 36 (2003): 368-372.
- Kano, Y.; Inoue, M.; Akiba, I.; Akiyama, S.; Sano, H.; and Fujita, Y. Effect of Substrate on Gradient Domain Morphology Formed in Acrylate Copolymer/Fluoro-copolymer Blends. Polymer 39 (1998): 6747-6745.
- Kealbe, D. H. Physical Chemistry of Adhesion., John Wiley and Sons, 1971.
- Kiefera, R. L.; Anderson, R. A.; Kim, M. H. Y.; and Thibeault, S. A. Radiation-cured polymeric nanocomposites of enhanced surface-mechanical properties. Nucl. Instrum. and Meth. B 208 (2003): 300-308.

- Kim, Y. S.; Yang, J.; Wang, S.; Banthia, A. K.; and McGrath, J. E. Surface and Wear Behavior of Bis-(4-hydroxyphenyl) Cyclohexane (bis-Z) Polycarbonate/Polycarbonate–Polydimethylsiloxane Block Copolymer Alloys. Polymer 43 (2002): 7207-7217.
- Kinloch, A.J. Adhesion and adhesives: science and technology, London: Chapman and Hall, 1987.
- Konieczny, M.; Xu, H.; Battaglis, R.; and Wunder, S. L. Curing Studies of The meta, para and 50/50 Mixed Isomers of The Ethyl Ester of 4,4'-Oxyaniline/Pyromellitic Dianhydride Polyamic Acid. Polymer 38 (1997): 2969-2979.
- Li, X.; Han, Y.; and An, L. Surface Morphology Control of Immiscible Polymer-blend Thin Films. Polymer 44 (2003): 8155-8165.
- Licari, J. J., and Hughes, L. A. Handbook of Polymer Coatings for Electronics Chemistry, Technology and Applications, New Jersey: Noyes Publications, 1990.
- Mochizuki, A.; Yamada K.; Ueda, M. ; and Yokota R. In situ Formed Three Layer Film by Isomerization of Fluorinated Polyisoimide in Polyethersulfone as a Matrix Polymer. Chem. Lett. 26 (1997): 333-334.
- Nah, C.; Han, S. H.; Lee, J. H.; Lim, S. D.; and Rhee, J. M. Intercalation Behavior of Polyimide/Organoclay Nanocomposites During Thermal Imidization. Composites Part B 35 (2004): 125-131.
- NASDA Rep. No. AU9-R02-K108 (2003).
- Ohya, H.; Kudryavtsev, V. V.; and Semenova, S. I. Polyimide Membranes. Tokyo: Kodanaha, 1996.
- Owen, M. J. Surface Chemistry and Applications. In Clarson, S. J. and Semlyen, J. A. (eds.), Siloxane Polymers, pp. 309-372. New Jersey: PRT Prentice Hall, 1993.
- Polk, W. D. Polydimethylsiloxane Containing Block Copolymers: Synthesis and Characterization of Alternating Poly(arylene Ether Phosphene Oxide)-b-Siloxane and Segmented Nylon 6,6–b-Siloxane Copolymers. Doctoral dissertation, Chemistry, Virginia Polytechnic Institute and State University, (2001).

- Rimdusit, S. and Yokota, R. Atomic Oxygen Protections in Polymeric Systems: A Review. J. Space Techn. Sci. 18 (2002): 34-48.
- Silverman, E.M. Environmental Effects on Spacecraft: LEO Materials Selection Guide NASA Contractor Report 4661 Part 1 and Part 2 (1995).
- Smith, G. L.; DeSimone, S. D.; Huang, J. M.; York, H.; Dwight, G.; Wilkes, D. W.; and McGrath, J. E. Synthesis and Characterization of Poly(methyl methacrylate)-g-poly(dimethylsiloxane) Copolymers. 1. Bulk and Surface Characterization. Macromolecules 25 (1992): 2575-2581.
- Spanos, C. G.; Ebbens, S. J.; Badyal, J. P. S.; Goodwin, A. J.; and Merlin, P. J. Surface Segregation and Plasma Oxidation of Polyethylene-Poly(dimethylsiloxane) Copolymer Doped Polyethylene Films. Macromolecules 36 (2003): 368-372.
- Tanaka, K.; Takahara, A.; and Kajiyama, T. Film Thickness Dependence of the Surface Structure of Immiscible Polystyrene/Poly(methyl methacrylate) Blends. Macromolecules 29 (1996): 3232-3239.
- Tiwari, A. and Nema, S. K. Synthesis, Characterization, Physicochemical and Dielectric Properties of Siloxane, Polyimide and Their Blends. Mat. Res. Innovant 7 (2003): 133-143.
- Tiwari, A.; Nema, S. K.; Das, C. K.; and Nema, S. K. Thermal Analysis of Polysiloxanes, Aromatic Polyimide and Their Blends. Thermochimica Acta 417, (2004): 133-142.
- Ton-That, C.; Shard, A. G.; Teare, D. O. H.; and Bradley, R. H. XPS and AFM surface studies of solvent-cast PS/PMMA blends. Polymer 42 (2001): 1121-1129.
- Walheim, S.; Boltau, M.; Mlynek, J.; Krausch, G.; and Steiner, U. Structure Formation via Polymer Demixing in Spin-Cast Films. Macromolecules 30 (1997): 4995-5003.
- Watson, K. A.; Ghoseb, S.; Delozierb, D. M.; Smith Jr, J. G.; and Connellb, J.W. Transparent, flexible, conductive carbon nanotube coatings for electrostatic charge mitigation. Polymer 46 (2005): 2076-2085.
- Wen, J.; Somorjai, G.; Lim, F.; and Ward, R. XPS Study of Surface Composition of a Segmented Polyurethane Block Copolymer Modified by PDMS End

- Groups and Its Blends with Phenoxy. Macromolecules 30 (1997): 7206-7213.
- Willson, D., Stenzenberger, H. D., and Hergenrother, P. M., eds. Polyimides. London: Blackie & Son Ltd, 1990.
- Winesett, D. A.; Ade, H.; Sokolov, J.; Rafailovich, M.; and Zhu, S. Substrate Dependence of Morphology in Thin Film Polymer Blends of Polystyrene and Poly(methyl methacrylate). Polym. Inter. 49 (2000): 458-462.
- Wu, S. Polymer Interface and Adhesion, New York: Marcel Dekker, (1982).
- Yamada, Y. Siloxane Modified Polyimides for Microelectronics Coating Applications. High Perform. Polym 10 (1998): 69-80.
- Yang, C. P and Su, Y. Y. Colorless polyimides from 2,3,3',4'-biphenyltetracarboxylic dianhydride (a-BPDA) and various aromatic bis(ether amine)s bearing pendent trifluoromethyl groups. Polymer 46 (2005): 5797-5807.
- Yokota, R. J. Recent Trends and Space Applications of Polyimides. Journal of Photopolymer Science and Technology 12 (1999): 209-216.
- Zisman, W. A., Jarvis, N. L., and Fox, R. B. Contact Angle, Wettability and Adhesion. Advances in chemistry series 43. Washington D.C.: American Chemical Society, 1964, p. 317. Cite in Bowens, A. D. Synthesis and Characterization of Poly(siloxane imide) Block Copolymers and End-Functional Polyimides for Interphase Applications. Doctoral dissertation, Chemistry, Virginia Polytechnic Institute and State University, (1999).
- Zuo, M.; Takeichi, T.; Matsumoto, A.; and Tsutsumi, K. Surface Characterization of Polyimide Films. Colloid & Polymer Sci 276 (1998): 555-564.



APPENDICES

สถาบันวิทยบริการ
จุฬาลงกรณ์มหาวิทยาลัย

APPENDIX A

Surface Characterization

Appendix A-1 Contact angle of s-BPDA/ODA polyimide film prepared at various temperature.

Treatment temperature (°C)	Contact angle (Degree)	
	Air side	Glass side
60	69	64
150	77	69
200	80	73
300	83	77

Appendix A-2 Water contact angle of s-BPDA/ODA polyimide, BSF30 and their blends as a function of BSF30 compositions.

BSF30 Composition (phr)	Contact angle (Degree)	
	Air side	Glass side
0 (s-BPDA/ODA)	82	78
0.5	102	77
1	102	76
2	101	77
3	102	77
4	102	78
5	102	77
30	104	78
100 (BSF30)	106	96

Appendix A-3 Ethylene glycol contact angle of s-BPDA/ODA polyimide, BSF30 and their blends as a function of BSF30 compositions.

BSF30 Composition (phr)	Contact angle (Degree)	
	Air side	Glass side
0 (s-BPDA/ODA)	62	58
0.5	83	59
1	83	58
2	83	58
3	83	58
4	82	58
5	83	59
30	83	58
100 (BSF30)	83	58

Appendix A-4 Surface tension of s-BPDA/ODA polyimide, BSF30 and their blends as a function of BSF30 compositions.

BSF30 Composition (phr)	γ_s^p (Dyne/cm)	γ_s^d (Dyne/cm)	γ_s (Dyne/cm)
0 (s-BPDA/ODA)	9.00	19.00	28.00
0.5	1.00	21.00	22.00
1	0.80	22.50	23.30
2	1.17	21.10	22.27
3	0.80	22.50	23.30
4	1.35	21.20	22.55
5	1.17	21.10	22.27
30	1.00	21.00	22.00
100 (BSF30)	0.20	21.60	21.80

Appendix A-5 Contact angle of 3 phr s-BPDA/ODA polyimide-BSF30 blends at various cosolvent compositions.

Side	Water Contact Angle (Degree) at			
	0% THF	50% THF	100% THF	150% THF
Air	101	101	102	102
Glass	77	77	77	77



สถาบันวิทยบริการ
จุฬาลงกรณ์มหาวิทยาลัย

APPENDIX B

Thermal Properties Characterization

Appendix B-1 The glass transition temperature of s-BPDA/ODA polyimide, BSF30 and there blends.

BSF30 Composition (phr)	Glass Transition Temperature (°C)
0 (s-BPDA/ODA)	274
0.5	272
1	269
2	270
3	268
4	270
5	273
30	166 (T _{g1}), 270 (T _{g2})
100 (BSF30)	165

สถาบันวิทยบริการ
จุฬาลงกรณ์มหาวิทยาลัย

Appendix B-2 The degradation temperature of s-BPDA/ODA polyimide, BSF30 and there blends.

BSF30 Composition (phr)	Degradation Temperature (°C)	
	5 wt% loss	10 wt% loss
0 (s-BPDA/ODA)	572	590
0.5	573	591
1	566	587
2	578	596
3	551	582
4	562	586
5	537	578
100 (BSF30)	430	451

* The degradation temperature of 30 phr (from DTG): 425°C and 610°C

Appendix B-3 The char yield of s-BPDA/ODA polyimide, BSF30 and there blends.

BSF30 Composition (phr)	Char Yield (%)
0 (s-BPDA/ODA)	60.36
0.5	59.62
1	59.92
2	58.81
3	58.39
4	58.92
5	57.81
30	53.73
100 (BSF30)	30.69

Appendix B-4 The glass transition temperature of s-BPDA/ODA polyimide, BSF30 and there blends at various cosolvent.

Cosolvent (%)	Glass Transition Temperature (°C)
0	266
50	267
100	268
150	268



สถาบันวิทยบริการ
จุฬาลงกรณ์มหาวิทยาลัย

APPENDIX C

Dynamic Mechanical Properties Characterization

Appendix C-1 The storage modulus of s-BPDA/ODA polyimide, BSF30 and there blends.

BSF30 Composition (phr)	Storage modulus at 30°C(GPa)
0 (s-BPDA/ODA)	2.95
0.5	2.75
1	2.68
2	2.65
3	2.60
4	2.60
5	2.67
30	1.70
100 (BSF30)	1.47

Appendix C-2 The glass transition temperature of s-BPDA/ODA polyimide, BSF30 and there blends (from DMA).

BSF30 Composition (phr)	Glass Transition Temperature (°C)
0 (s-BPDA/ODA)	285
0.5	280
1	268
2	280
3	268
4	255
5	260
100 (BSF30)	155

APPENDIX D

Mechanical Properties Characterization

Appendix D-1 Mechanical properties of s-BPDA/ODA polyimide, BSF30 and there blends.

BSF30 Composition (phr)	Tensile Modulus (GPa)	Tensile strength (MPa)
0 (s-BPDA/ODA)	2.64	138
0.5	2.41	109
1	2.00	112
2	2.25	126
3	2.18	123
4	1.98	109
5	2.08	130
30	1.43	65
100 (BSF30)	1.05	43

สถาบันวิทยบริการ
จุฬาลงกรณ์มหาวิทยาลัย

VITA

Ms. Wanpen Benjapan was born in Surattanee, Thailand on May 19, 1980. She graduated at high school level in 1998 from Chulaporn Collage School. She received the Bachelor's Degree of Engineering with a major in Chemical Engineering from the Faculty of Engineering, Srinakarintarawirot Ongkarak University in 2002. After graduation, she entered study for a Master's Degree of Chemical Engineering at the Department of Chemical Engineering, Faculty of Engineering, Chulalongkorn University.



สถาบันวิทยบริการ
จุฬาลงกรณ์มหาวิทยาลัย